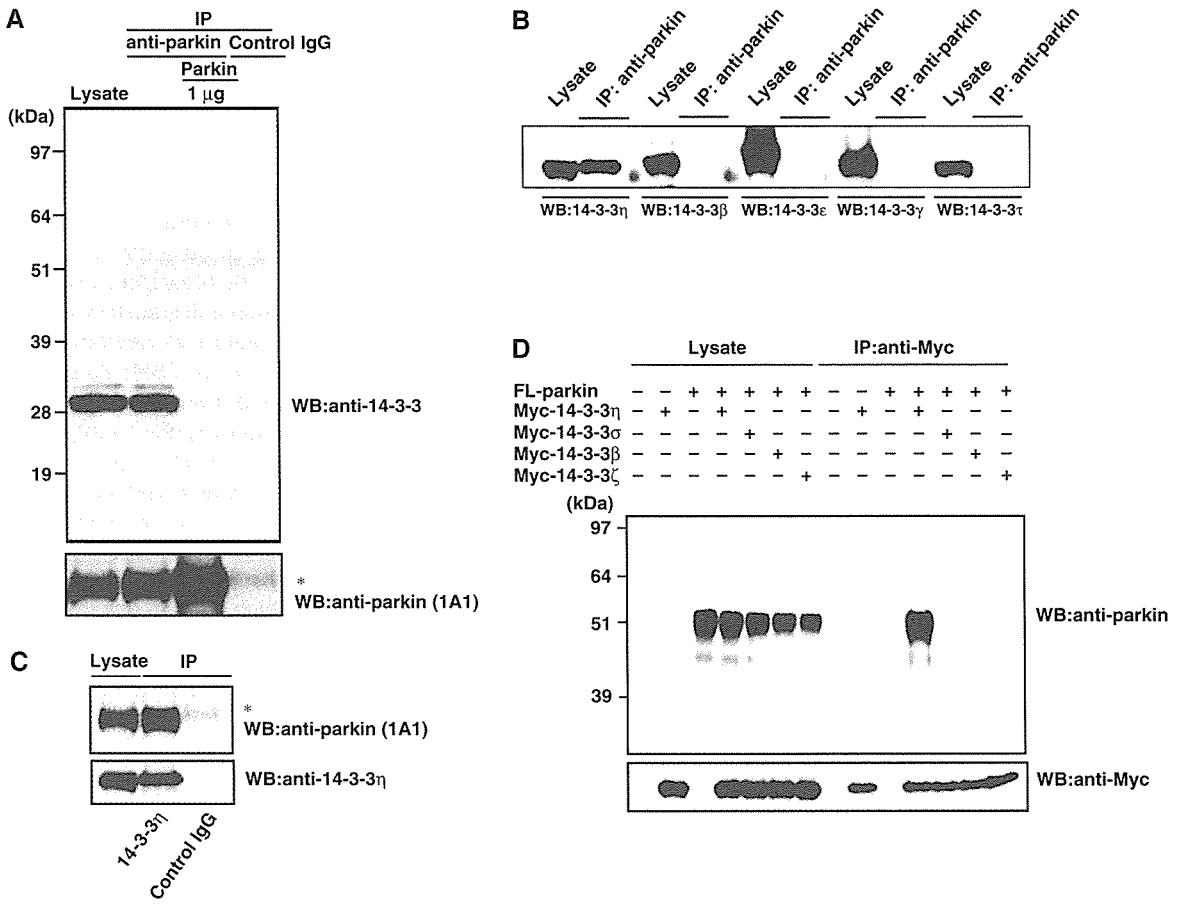

Figure 1 Physical interaction between parkin and 14-3-3η. (**A**) Immunoprecipitation by anti-parkin antibody in the mouse brain. Mouse brain lysates were prepared and treated with anti-parkin or control IgG as described in Materials and methods. The resulting immunoprecipitates were subjected to SDS–PAGE, followed by Western blotting with anti-14-3-3 and parkin (1A1) antibodies. In all, 1 μg of recombinant parkin was pretreated with anti-parkin prior to immunoprecipitation. Left lane: the brain lysate (1.5% input). Asterisk denotes an IgG heavy chain. (**B**) Specificity analysis of 14-3-3 species. The immunoprecipitation with anti-parkin and subsequent SDS–PAGE were carried out as in (A). Western blotting was conducted with antibodies against various 14-3-3 isoforms as indicated for lysates and anti-parkin immunoprecipitates. (**C**) Immunoprecipitation by anti-14-3-3η antibody. After immunoprecipitation with anti-14-3-3η or control IgG of the brain lysate, the immunoprecipitates were analyzed by Western blotting with anti-parkin (1A1) and 14-3-3η antibodies, similar to (A). Left lane: the brain lysate (1.5% input). Asterisk denotes an IgG heavy chain. (**D**) Interaction between parkin and 14-3-3η in HEK293 cells. FL-parkin (5 μg), Myc-14-3-3η, σ, β, or ζ (2 μg) plasmids were transfected as indicated into HEK293 cells. After 48 h, the cell lysate was prepared and used for immunoprecipitation with anti-Myc antibody. The immunoprecipitates and the lysate (7.5% input) were analyzed by Western blotting with anti-parkin and Myc antibodies, as in (A).

with recombinant parkin protein (1 μg). Intriguingly, two 14-3-3 signals were evident: a faint band and a strongly stained band, indicating that the 14-3-3 may form homo- and/or hetero-dimers. Subsequently, we determined the type(s) of 14-3-3 species that interacts with parkin in the mouse brain in more detail. In the parkin immunoprecipitant, 14-3-3η, but not other 14-3-3 isoforms examined, that is, β, γ, ε, and τ, was detected (Figure 1B). In the next step, we examined whether parkin is coimmunoprecipitated with anti-14-3-3η antibody and found parkin in the 14-3-3η immunoprecipitant (Figure 1C). These reciprocal immunoprecipitation experiments revealed that parkin is associated with 14-3-3η in the mouse brain.

To confirm the specific interaction of parkin with 14-3-3η, Myc-tagged 14-3-3η, σ, β, or ζ was cotransfected with FLAG (FL)-parkin into HEK293 cells, and their interactions were tested. FL-parkin was detected in the immunoprecipitant of Myc-14-3-3η, but not those of Myc-14-3-3σ, β, and ζ (Figure 1D). Taken together with the results of Figure 1B, our data indicate that parkin mainly interacts with 14-3-3η.

Parkin domain interacts with 14-3-3η

We next investigated the region of parkin necessary for interaction with 14-3-3η. Structurally, parkin is characterized by the presence of the N-terminal ubiquitin-like domain (UBL) (which is highly homologous to ubiquitin), the C-terminal RING box, consisting of two RING finger motifs, RING1 and RING2, flanked by one IBR (in between RING finger) motif, and a linker region, which connects these N- and C-terminal regions (Shimura *et al*, 2000). In these experiments, various deletion mutants of FL-tagged parkin were expressed in HEK293 cells and immunoprecipitated by FL-antibody beads (Figure 2A). FL-parkin or its derivatives on the beads were further incubated with cell lysates that expressed Myc-14-3-3η, and then the amounts of Myc-14-3-3η bound to the beads were determined (Figure 2B).

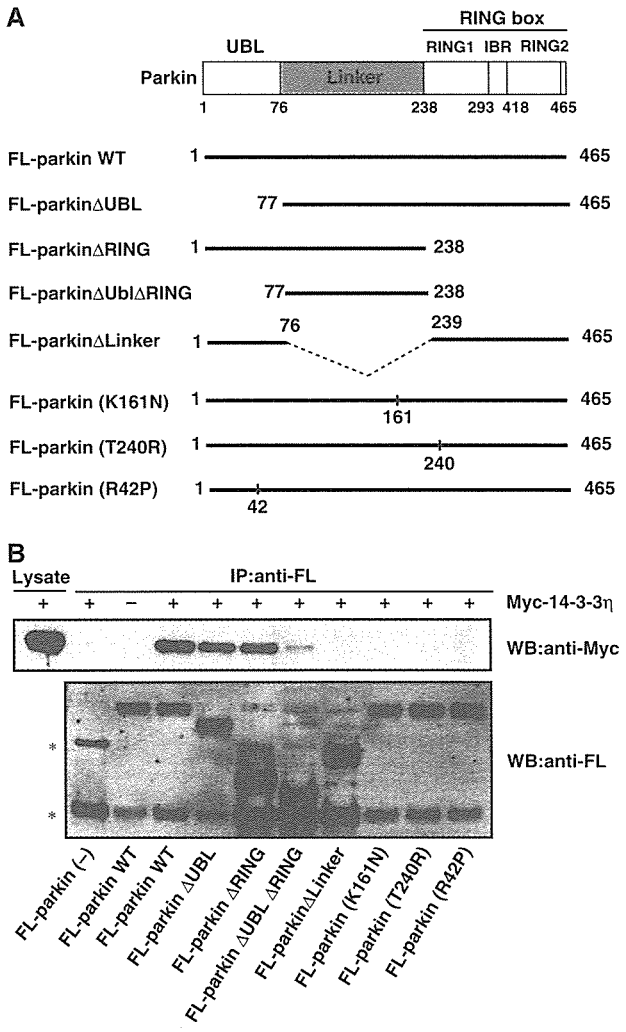

Figure 2 Domain analysis of the parkin region that interacts with 14-3-3η. (**A**) Schematic representation of WT parkin and its deletion- and disease-related missense mutants. See text for the domain structures of parkin and mutants. The dotted line denotes the deleted region. (**B**) Interaction between 14-3-3η and parkin mutants. FL-parkin (2 μg) or its mutant (10 μg) plasmids were transfected into HEK293 cells, as described in Figure 1D. The cell lysates (200–600 μl) were immunoprecipitated with anti-FL-antibody beads. Note that various amounts of the lysates were used to adjust roughly the levels of expressed parkin mutants. The resulting immunoprecipitates were mixed with other cell lysates (200 μl) prepared from cells that had been transfected with Myc-14-3-3η plasmid (2 μg) and incubated for 6 h at 4°C. Then, the extensively washed immunoprecipitates and cell lysate (7.5% input) were analyzed by Western blotting with anti-Myc and FL antibodies. Asterisks denote nonspecific bands.

The full-length parkin could bind 14-3-3η. Deletion of either UBL or RING-box domain reduced the binding compared to the full-length parkin, although these deletion mutants retained the ability to bind to 14-3-3η. Furthermore, mutants with combined deletions of the UBL and RING-box domains, that is, the linker region, could also bind 14-3-3η to a lesser extent. Conversely, deletion of the linker region resulted in the loss of ability to bind 14-3-3η. Taken together, it is concluded that the linker region is necessary for the interaction between parkin and 14-3-3η, although the UBL and RING-box domains may enhance the binding affinity.

Interestingly, the ARJP disease-causing missense mutation within the linker region, that is, parkin(K161N), in which the Lys residue at position 161 was replaced by Asn residue, showed complete loss of binding to 14-3-3η, confirming the importance of the linker region in the interaction between 14-3-3η and parkin. Unexpectedly, other disease-causing missense mutations of the UBL region, parkin(R42P), and the RING1 region, parkin(T240R), also showed complete loss of interaction with 14-3-3η (Figure 2). Thus, although the UBL and RING-box domains are not primarily required for the binding, both R42P and T240R mutations in the UBL and RING-box domains, respectively, deleteriously affect the neighboring linker domain. Alternatively, since 14-3-3 is known to form a homo- or hetero-dimer, and thus has two binding sites (Aitken *et al*, 2002), it is plausible that 14-3-3η interacts with two distinct regions of parkin, one major site of which is the linker region.

Effect of suppression of 14-3-3η on parkin E3 activity

We next investigated the role of parkin–14-3-3η binding on parkin activity. At first, we tested its effect on the ubiquitin ligase activity of parkin. We incubated recombinant His-parkin with ubiquitin, E1, and E2 (UbcH7) *in vitro*. Under this condition, His-parkin appeared as a smear band, which likely reflects self-ubiquitylation (Figure 3A). Addition of recombinant GST-14-3-3η (Figure 3A, left panel) or untagged 14-3-3η (Figure 3A, right panel) to the reaction reduced the smear of His-parkin, and such reduction was proportionate to the added amount of GST-14-3-3η or 14-3-3η and resulted in the recovery of His-parkin of intact size. In addition, we found that 14-3-3η had no effect on the ubiquitylating activity of phosphorylated IκBα by a fully *in vitro* reconstituted system, containing E1, E2 (Ubc4), and E3 (the $SCF^{\beta TrCP}$ complex; Kawakami *et al*, 2001), indicating that 14-3-3η does not interfere with ubiquitylating reactions in general (data not shown). These results strongly suggest that 14-3-3η suppresses the intrinsic self-ubiquitylation activity of parkin.

We next tested whether 14-3-3η also affects the ubiquitylation activity of parkin in HEK293 cells. First, we examined the self-ubiquitylation of parkin, whose activity was observed by cotransfections of HA-ubiquitin and FL-parkin. Myc-14-3-3η almost completely suppressed the self-ubiquitylation activity of parkin, while Myc-14-3-3σ, β, and ζ had no inhibitory effect (Figure 3B), indicating the specific role of 14-3-3η for parkin. Second, we examined the effect of 14-3-3η on the ubiquitylation of a model substrate for parkin. When V5-tagged synphilin-1, a known parkin substrate (Chung *et al*, 2001), was transfected with FL-parkin and HA-ubiquitin in the cells, V5-synphilin-1 was found in ubiquitylated form, as demonstrated by the poly-ubiquitin chain formation (detected by anti-HA antibody) in anti-V5 immunoprecipitant (Figure 3C, top panel). V5-synphilin-1 was not ubiquitylated when FL-parkin was not cotransfected, suggesting that this ubiquitylation is mediated by coexpressed FL-parkin. Indeed, FL-parkin was found to be associated with V5-synphilin-1, further supporting the above notion (Figure 3C, second panel from the top). Note that the polyubiquitylated bands observed as the smear profile were considered to include not only major synphilin-1 bands over 90-kDa size but also self-ubiquitylated bands of parkin over 52-kDa size.

In the next step, we tested the effects of 14-3-3η on the ubiquitylation and binding activities of parkin to

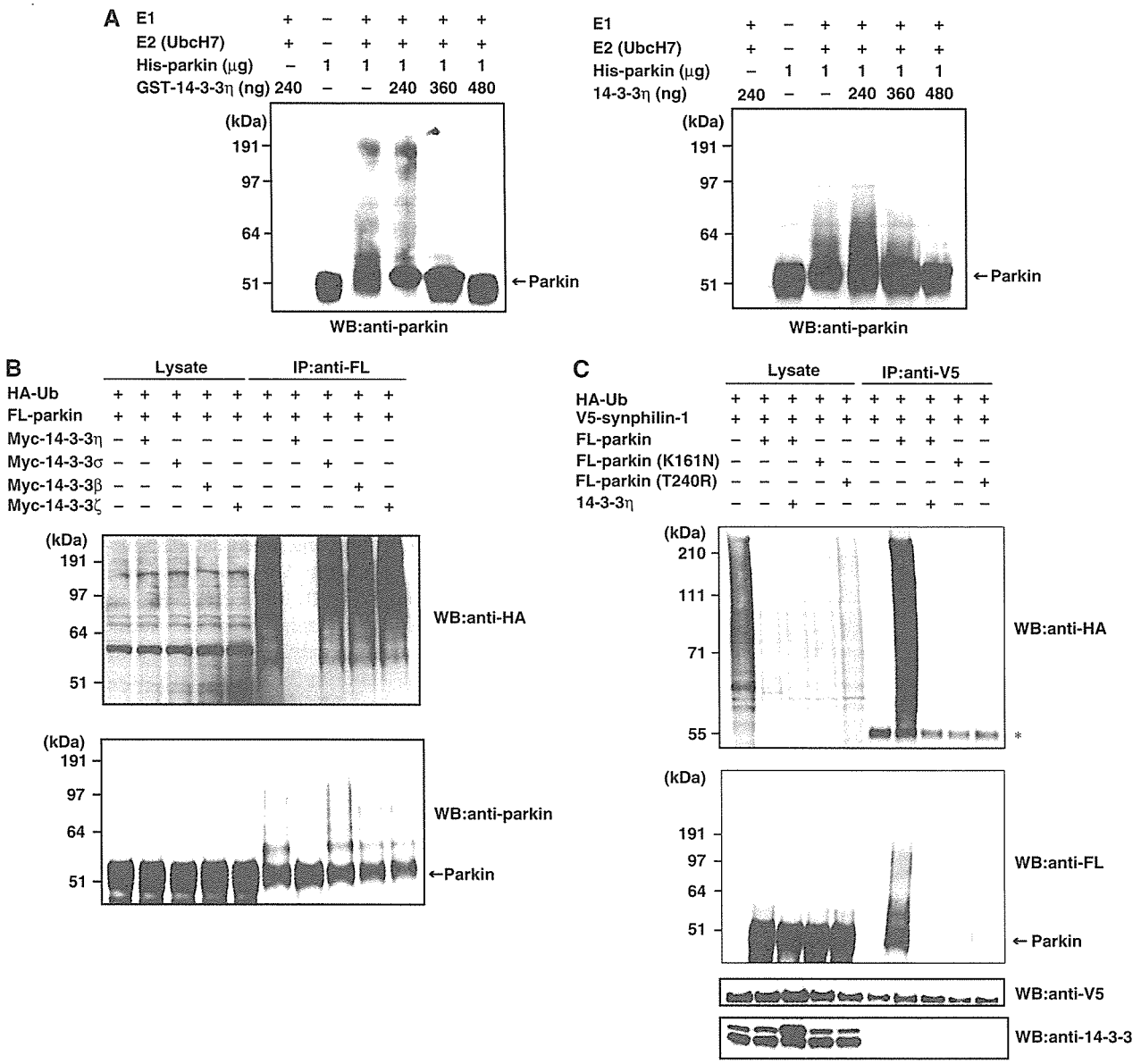

Figure 3 Effects of 14-3-3η on the E3 activity of parkin. (**A**) *In vitro* autoubiquitylation. The ubiquitylating assay was conducted as described in Materials and methods with or without various amounts of GST-14-3-3η (left panel) or 14-3-3η (right panel). After incubation, the reaction mixtures were subjected to SDS–PAGE, followed by Western blotting with anti-parkin. Arrow on the right indicates the position of His-parkin. (**B**) *In vivo* autoubiquitylation. HA-Ub (3 μg), FL-parkin (3 μg), and Myc-14-3-3η, σ, β, or ζ (6 μg) plasmids were transfected for 48 h into HEK293 cells as indicated. After immunoprecipitation with anti-FL, Western blotting was performed using antibodies against HA and parkin. Western blotting of all lysates was performed to test the expression levels (Lysate). (**C**) Ubiquitylation of synphilin-1 in HEK293 cells. HA-Ub (2 μg), FL-parkin (3 μg), FL-parkin(K161N) (3 μg), FL-parkin(T240R) (3 μg), Myc-14-3-3η (6 μg), and V5-synphilin-1 (4 μg) plasmids were transfected into HEK293 cells as in (B) at the indicated combinations. After immunoprecipitation with anti-V5 antibody, Western blotting was performed using antibodies against HA, FL, V5, and 14-3-3. Asterisk denotes an IgG heavy chain.

V5-synphilin-1. Cotransfection of 14-3-3η resulted in almost complete inhibition of the ubiquitylation of synphilin-1 by parkin and/or self-ubiquitylation of parkin (Figure 3C, top and second panels), as well as inhibition of the interaction between synphilin-1 and parkin (Figure 3C, second panel). 14-3-3η did not interact with synphilin-1 (Figure 3C, bottom panel). Taken together, these results suggest that 14-3-3η does not only inhibit the intrinsic ubiquitylation activity of parkin, but also its binding activity to the substrate and its ubiquitylation.

The ARJP disease-related parkin(K161N) and parkin(T240R) mutants, which cannot bind with 14-3-3η, could not bind and ubiquitylate synphilin-1 and/or self-ubiquitylation of parkin even in the absence of 14-3-3η (Figure 3C, top panel). Hence, the linker and RING-box domains of parkin are essential not only for the negative regulation by 14-3-3η, but also for the substrate recognition and ubiquitin-ligase activity. These results illustrate the importance of these regions of parkin on its positive and negative regulation.

Since parkin is known to associate with E2 (Shimura *et al*, 2000), we also examined the effect of 14-3-3η on the ability of parkin to recruit E2. For this purpose, we coexpressed HA-parkin with FL-UbcH7 or FL-Ubc7, both of which are known

to bind to parkin (Shimura *et al* 2000; Imai *et al*, 2001). Almost the same amounts of UbcH7 (Figure 4A) and Ubc7 (Figure 4B) were detected in the anti-parkin immunoprecipitants irrespective of cotransfection with Myc-14-3-3η. These findings indicate that 14-3-3η does not influence the recruitment of E2, that is, UbcH7 or Ubc7, to parkin.

α-Synuclein abrogates 14-3-3η-related parkin inactivation

Based on the above findings, we next examined the mechanism that regulates the 14-3-3η–parkin binding. As α-SN partly has a high homology to 14-3-3 isoforms (Ostrerova *et al*, 1999), we tested the effects of α-SN on the 14-3-3η-induced suppression of parkin. By cotransfection experiments in HEK293 cells, parkin again ubiquitylated synphilin-1, and 14-3-3η inhibited the parkin-mediated ubiquitylation (Figure 5A). Coexpression of α-SN resulted in the recovery of ubiquitylation of synphilin-1 and the association of synphilin-1 with parkin, suggesting that α-SN abrogates the 14-3-3η-induced suppression of parkin (Figure 5A, top panel). Importantly, the familial PD-related mutants of α-SN(A30P) (Kruger *et al*, 1998) and α-SN(A53T) (Polymeropoulos *et al*, 1997) could not abrogate the inhibitory role of 14-3-3η. Similar results were observed by detection of self-ubiquitylation activity of parkin (Figure 5A, second panel).

We then tested whether α-SN can release the binding of Myc-14-3-3η from parkin in cotransfection experiment. As shown in Figure 5B (top panel), FL-parkin was self-ubiquitylated in the absence of 14-3-3η. Coexpression of 14-3-3η inhibited the self-ubiquitylation of parkin, and this was accompanied by the binding of 14-3-3η to FL-parkin. Coexpression of α-SN abrogated the binding of 14-3-3η to parkin and resulted in the recovery of self-ubiquitylation of parkin. These effects were not seen by coexpression of α-SN(A30P) and α-SN(A53T) (Figure 5B, top panel). In addition, while the 14-3-3η–parkin interaction was considerably reduced by α-SN, it was not reduced by α-SN(A30P) or α-SN(A53T) (Figure 5B, bottom panel). Taken together, α-SN, but not α-SN(A30P) or α-SN(A53T), binds strongly to 14-3-3η and thereby releases parkin from the parkin–14-3-3η complex.

We also tested the interaction of Myc-14-3-3η with FL-α-SN, FL-α-SN(A30P), and FL-α-SN(A53T). Myc-14-3-3η interacted only with FL-α-SN, but not α-SN(A30P) nor α-SN(A53T) (Figure 5C, upper-top panel), suggesting that α-SN relieves parkin activity from binding to 14-3-3η. The 14-3-3η/α-SN interaction was not affected by parkin (Figure 5C, upper-top panel), and parkin was not associated with α-SN (Figure 5C, upper-second panel). Interestingly, FL-α-SN did not interact with Myc-14-3-3σ, β, and ζ in the same experiment (Figure 5C, lower panel). These results further strengthen the notion that α-SN specifically activates parkin through binding 14-3-3η.

We then investigated whether the interaction of 14-3-3η and parkin is direct or indirect by using purified recombinant His-parkin and GST-14-3-3η. GST or GST-14-3-3η was mixed with His-parkin, and pulled down by glutathione beads. His-parkin bound to GST-14-3-3η, but not GST (Figure 5D, left panel), indicating that parkin directly interacts with 14-3-3η. On the other hand, a similar *in vitro* binding assay showed that GST-14-3-3η did not interact with recombinant α-SN (Figure 5D, right panel), suggesting that certain modification(s) of α-SN may be required for the interaction of 14-3-3η.

Subsequently, we measured the binding affinities of parkin and α-SN for 14-3-3η by the surface plasmon resonance (SPR) method. As shown in Figure 5E, parkin bound 14-3-3η with a considerably strong affinity ($K_d = 4.2$ nM, upper), whereas the affinity of α-SN for 14-3-3η was much lower than that of parkin ($K_d = 1.1$ μM, lower). These results are consistent with those of the immunoprecipitation/Western analysis using recombinant proteins (Figure 5D).

Finally, we examined whether 14-3-3η bound to parkin can be released by α-SN. To test this, we first mixed the lysates coexpressing FL-parkin and Myc-14-3-3η of HEK293 cells with those expressing α-SN. Then the mixtures were incubated under three different conditions, as indicated in the upper panel of Figure 5F. Next, the lysates were immunoprecipitated with anti-FL antibody, and followed by Western blotting with anti-Myc and anti-parkin antibodies. As shown in Figure 5F (upper panel), the amount of 14-3-3η bound to parkin was significantly lower in all incubation conditions, when the cell lysates that simultaneously expressed both parkin and 14-3-3η were incubated with α-SN-expressing lysates. Incubation for 1 h at 37°C reduced the amount of 14-3-3η bound to parkin in proportion to the added amount of α-SN-expressing cell lysate (Figure 5F, lower panel). Intriguingly, the α-SN(A30P) and α-SN(A53T) mutants had no effect on the release of 14-3-3η, unlike wild-type (WT) α-SN (Figure 5F, lower panel). These observations strongly indicate that α-SN, but not α-SN(A30P) or α-SN(A53T), can capture and release 14-3-3η from the parkin–14-3-3η complex, which supports our notion that the negative regulation of parkin activity by 14-3-3η is relieved by α-SN (Figure 5A and B).

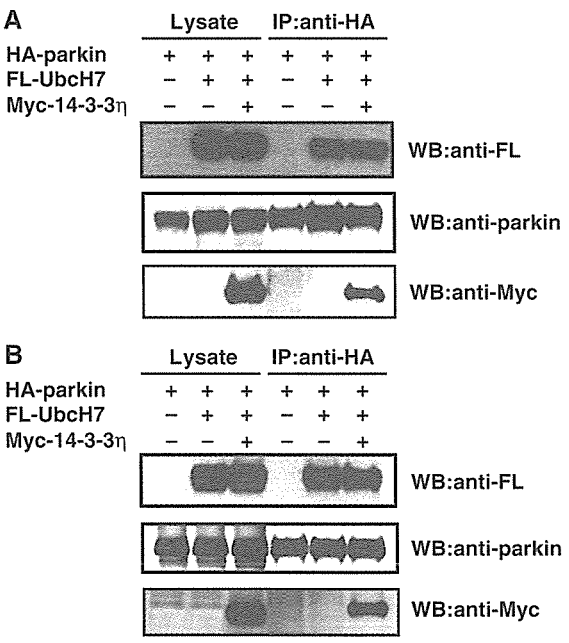

Figure 4 Effect of 14-3-3η on the recruitment of E2 (UbcH7 or Ubc7) to parkin. (**A**) HA-parkin (3 μg), FL-UbcH7 (3 μg), or Myc-14-3-3η (6 μg) plasmids were transfected for 48 h into HEK293 cells at the indicated combinations. After immunoprecipitation with anti-HA antibody, Western blotting was performed using antibodies against FL, Myc, and parkin. (**B**) The experiment was conducted as in (A), except that FL-Ubc7 was used instead of FL-UbcH7.

Parkin, 14-3-3η, and α-SN levels in the substantia nigra of PD

Finally, we analyzed the levels of parkin, 14-3-3η, and α-SN in the substantia nigra of the midbrain from patients with sporadic PD. Western blotting revealed no significant differences in parkin, 14-3-3η, and actin in the substantia nigra between control (patients without PD) and PD patients, whereas α-SN was significantly increased in the substantia nigra of PD patients (Figure 6A, upper panel). As parkin did not interact physically with α-SN in our immunoprecipitation analysis (Figure 5C; data not shown), we then examined the interactions of 14-3-3η with parkin or α-SN by measuring

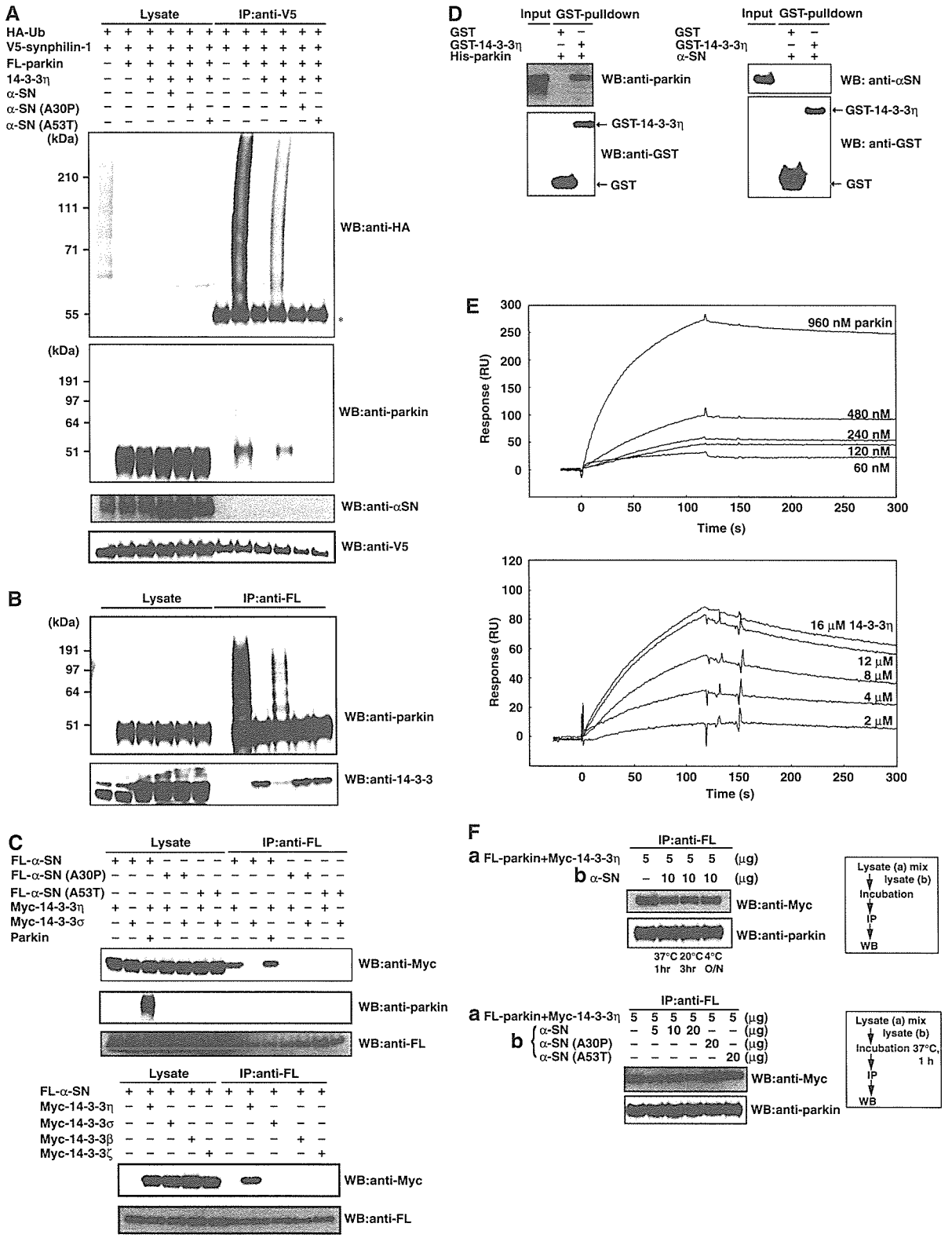

these proteins in the anti-14-3-3η immunoprecipitant. Whereas the levels of parkin associated with 14-3-3η from PD appeared to be decreased relative to the control, the levels of α-SN that interacted with 14-3-3η were clearly increased in patients with PD (Figure 6A, lower panel). Thus, it is suggested that the elevated levels of α-SN are associated with its interaction with 14-3-3η and the activity of parkin may be aberrantly regulated in the substantia nigra of sporadic PD.

Discussion

The major finding of the present study was the identification of 14-3-3η as a novel regulator of parkin. First, parkin was in a complex with 14-3-3η, but not β, γ, ε, or τ isoforms, in the mouse brain (Figure 1). 14-3-3η could bind primarily to the linker region of parkin, but not with the ARJP-causing missense mutant parkin (K161N), which has a mutation in the

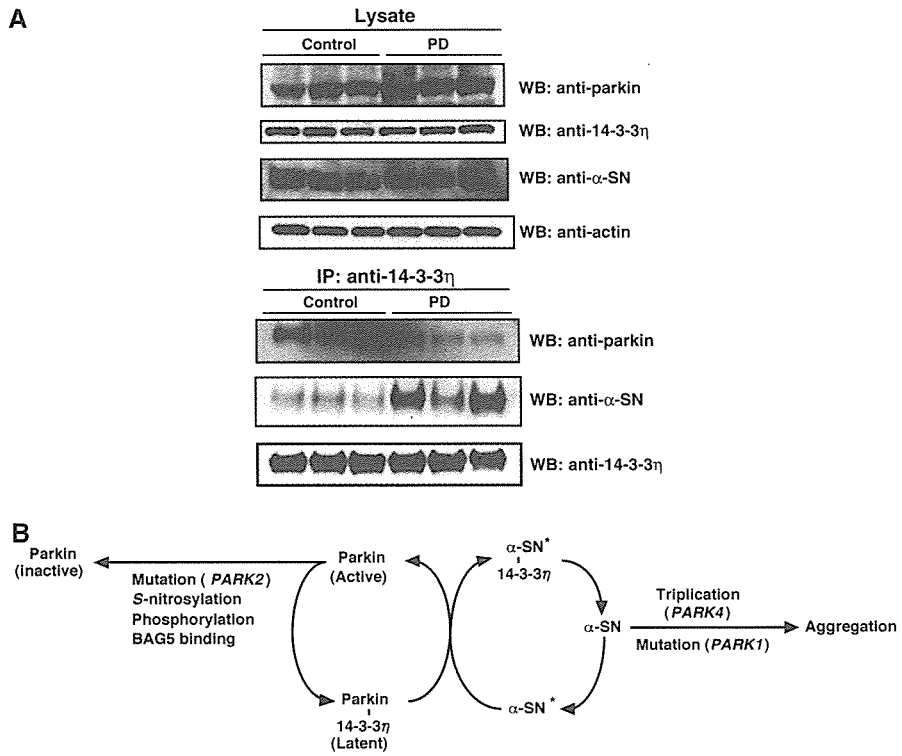

Figure 6 (**A**) Levels of parkin, 14-3-3η, and α-SN in the substantia nigra of PD. Brain of a representative patient with PD (upper panel). Samples (30 μg) of the crude extract of the brains (substantia nigra) of control (patients without PD) and PD patients were subjected to SDS–PAGE, following Western blotting against antibodies against parkin, 14-3-3η, α-SN, and actin. Physical interaction between 14-3-3η and parkin or α-SN (lower panel). After the same samples used in the upper panel were immunoprecipitated with anti-14-3-3η, Western blotting was carried out using antibodies against parkin, α-SN, and 14-3-3η. (**B**) A schematic diagram showing the pathways involved in the regulation of parkin activity by 14-3-3η and α-SN. α-SN, α-synuclein; α-SN*, modified form of α-SN. Note that whether parkin is phosphorylated to bind to 14-3-3η remains unknown at present. See text for details.

Figure 5 Effects of α-SN on 14-3-3η-induced suppression of parkin E3 activity and interaction between 14-3-3η and α-SN in HEK293 cells. (**A**) Ubiquitylation of synphilin-1. Transfection was conducted at various combinations, as in Figure 3C, except for cotransfection of 4 μg of α-SN, α-SN(A30P), and α-SN(A53T). After immunoprecipitation with anti-V5 antibody, Western blotting was carried out with antibodies against HA, parkin and α-SN, and V5. Asterisk denotes an IgG heavy chain. (**B**) Autoubiquitylation of parkin. Transfection was performed as in (A). After immunoprecipitation with anti-FL antibody, Western blotting was carried out with antibodies against parkin and 14-3-3. (**C**) Interaction of 14-3-3η and α-SN with or without parkin. Various expression vectors at the indicated combinations were transfected. Immunoprecipitation was conducted by anti-FL antibody and the resulting immunoprecipitates were used for Western blotting with antibodies against Myc, parkin, and FL. (**D**) Physical interaction between 14-3-3η and parkin (left panel) or α-SN (right panel) in recombinant proteins. After recombinant His-tagged parkin produced from baculovirus-infected HiFive insect cells (3 μg) or GST-α-SN expressed in *E. coli* whose GST moiety was removed by PreScission Protease digestion prior to use (3 μg) was incubated for 1 h at 32°C with 3 μg of GST or GST-tagged 14-3-3η expressed in *E. coli*, glutathione-Sepharose was added and the incubation vessels were slowly rotated for 3 h at 4°C. The washed Sepharose resin was eluted with 50 μl of 50 mM Tris–HCl (pH 8.0) buffer containing 10 mM reduced glutathione, and aliquots (15 μl) were analyzed by Western blotting with antibodies against parkin (left-top panel), α-SN (right-top panel), and GST (bottom panel). Input: 500 ng of parkin or α-SN. (**E**) SPR analyses of parkin and α-SN binding to 14-3-3η. Upper: subtracted sensorgrams of interaction between a subset of parkin concentrations and immobilized 14-3-3η. Lower: subtracted sensorgrams of interaction between a subset of 14-3-3η concentrations and immobilized α-SN. (**F**) Sequestration of 14-3-3η by α-SN from the parkin–14-3-3η complex. Various expression vectors were transfected as indicated. Upper panel: 5 μg of the lysate-(a) from cells co-expressing FL-parkin and Myc-14-3-3η were mixed with 10 μg of cellular lysate-(b) expressing α-SN. The mixtures were incubated under various conditions; that is, 37°C for 1 h, 20°C for 3 h, or overnight at 4°C (O/N), then immunoprecipitation by anti-FL antibody was conducted, followed by Western blotting with antibodies against Myc (14-3-3η) and parkin. Lower panel: the experiments were conducted as for the top panel, except that incubation was carried out at 37°C for 1 h using α-SN-, α-SN(A30P)-, or α-SN (A53T)-expressing lysates as indicated. The experimental protocol is shown in the flow charts on the right.

linker region (Figure 2). Second, the binding of 14-3-3η to parkin was associated with suppression of the ubiquitin-ligase activity, suggesting that certain parkin bound to 14-3-3η is present at a latent status in the brain (Figure 3). Third, overexpression of α-SN abrogated the 14-3-3η-induced suppression of parkin activity, indicating that α-SN relieves the negative regulation of parkin by 14-3-3η (Figure 5A and B). Intriguingly, PD-causing A30P and A53T mutations of α-SN could not bind 14-3-3η and failed to activate parkin. These results indicate that 14-3-3η is a regulator that functionally links parkin and α-SN, as illustrated in Figure 6B.

It is of particular note that we report unusual isoform specificity for 14-3-3η to interact with parkin among all 14-3-3 species examined. However, the possibility that the other species are also involved in the interaction by forming a heterodimer with 14-3-3η cannot be excluded *in vivo*, because 14-3-3 bands immunoprecipitated by anti-parkin antibody from the brain extracts showed doublet with one weak signal for Western blotting (Figure 1A). Nevertheless, herein we address that recombinant parkin could directly bind to 14-3-3η (Figure 5D, left panel), with considerably high affinity (K_d = approximately 4 nM) (Figure 5E) and that the 14-3-3η homodimer is a negative factor for autoubiquitylating activity of parkin *in vitro* (Figure 3A).

It is known that the 14-3-3 family proteins interact with the majority, but not all, proteins after their phosphorylation (Aitken *et al*, 2002; Bridges and Moorhead, 2004; Mackintosh, 2004). Indeed, parkin contains the RKDSPP sequence in the linker region that resembles the typical binding motifs with a potential phosphorylation residue for 14-3-3 proteins (Yaffe *et al*, 1997; Mackintosh, 2004). It is also known that parkin has several possible phosphorylation sites, and recent studies showed that parkin is phosphorylated *in vitro* (Yamamoto *et al*, 2004), although there is no direct evidence demonstrating phosphorylation of parkin *in vivo* to date. However, it remains elusive whether or not phosphorylation of parkin is responsible for its specific binding to 14-3-3η, because known potential phosphorylation motifs are capable of associating with many 14-3-3 species in general. The specificities of 14-3-3: client–protein interactions do not result from different specificities for the phosphopeptide-binding motifs, but probably arises from contacts made on the variable surface of 14-3-3 outside the binding cleft, as discussed previously by Yaffe *et al* (1997). In this regard, some reports showed functional specificities of 14-3-3 isoforms (Aitken, 2002; Aitken *et al*, 2002; Roberts and de Bruxelles, 2002), and indeed several enzymes retain several nonphosphorylated binding motifs for 14-3-3s (Hallberg, 2002; Sribar *et al*, 2003), though parkin lacks such 14-3-3-interacting sequences. Thus, parkin, in particular its linker region, may have a new binding motif(s) for 14-3-3η, but the interacting motif(s) remains to be identified. If 14-3-3η binds to parkin through two sites as a dimmer, it is plausible that the phosphorylation of parkin is involved in their interactions at least in part.

With regard to the mechanistic action of 14-3-3η, it may suppress parkin activity by preventing access of the substrate, because the binding of synphilin-1 (used here as a model substrate to parkin) was inhibited by 14-3-3η (Figure 3C). Accumulating evidence suggests that parkin can bind various targets by the UBL domain or the RING box, in particular the RING 1 domain (Dawson and Dawson, 2003). Accordingly, 14-3-3η may have function(s) other than suppressing the access of the substrate to parkin. Indeed, 14-3-3η strongly inhibits substrate-independent self-ubiquitylation of parkin, indicating blockage of the intrinsic E3 activity. It was also anticipated that 14-3-3η hinders the recruitment of E2 to parkin. However, this was not the case, because 14-3-3η had no effect on the binding of UbcH7 and Ubc7 to parkin (Figure 4). Thus, while the mechanism of 14-3-3η-induced suppression of parkin activity remains to be identified, it is possible that it involves preventing the positioning of the ubiquitin-charged E2 toward the target Lys residue by steric hindrance due to the association of 14-3-3η to parkin.

It is worth noting that parkin does not interact with α-SN directly, because we could not demonstrate the physical binding of parkin to α-SN *in vivo* and *in vitro* (data not shown; see also Dawson and Dawson, 2003). Nevertheless, we found that the negative regulation of parkin by 14-3-3η was relieved by α-SN, which could bind tightly to 14-3-3η *in vivo* (Figure 5A–C). In this regard, it is of note that the amounts of 14-3-3η bound to parkin were decreased when the lysates of cells coexpressing parkin and 14-3-3η were incubated with those expressing WT α-SN, but not PD-related α-SN(A30P) or α-SN(A53T) mutants *in vitro* (Figure 5F). These results clearly indicate that 14-3-3η bound to parkin is sequestered by α-SN, but not competition by α-SN toward the binding of 14-3-3η to parkin. Unlike the association between parkin and 14-3-3η, there is little or no interaction between α-SN and 14-3-3η *in vitro*, as recombinant α-SN did not bind to 14-3-3η (Figure 5D, right panel, and E). Thus, it is plausible that certain modification(s) of α-SN is required for its association to 14-3-3η in mammalian cells (see our model in Figure 6B). Judging from the characteristic properties of 14-3-3 family proteins capable of binding many phosphorylated proteins (Yaffe *et al*, 1997), certain phosphorylation(s) of α-SN seems quite possible for the interaction with 14-3-3η. Indeed, there are several reports regarding phosphorylation of α-SN (Fujiwara *et al*, 2002; Hirai *et al*, 2004). Although previous studies clearly demonstrated that α-SN deposited in synucleinopathy brains is extensively phosphorylated at Ser-129 (Fujiwara *et al*, 2002; Hirai *et al*, 2004), this is probably not the case in our study, because the chemically synthesized peptide phosphorylated at Ser-129 of α-SN did not bind to the 14-3-3η (our unpublished results). However, the possibility that α-SN is phosphorylated at other site(s) cannot be exclusively ruled out. Alternatively, one cannot exclude a possible, though yet unknown, modification(s) of α-SN other than phosphorylation as a mechanism responsible for the increased affinity toward 14-3-3η. In this regard, α-SN is structurally related to 14-3-3 family proteins (Ostrerova *et al*, 1999), but it is unknown whether the homologous region is involved in the physical interaction with α-SN. Further studies are required to clarify the mode of α-SN modification.

In the present study, we found reciprocal regulation of parkin activity by α-SN and 14-3-3η, whose tripartite control could enhance our understanding of the pathogenesis of PD. As illustrated in Figure 6B, to date there are several reports on the post-translational modification of parkin. Recent findings indicate that the ubiquitin E3 ligase activity of parkin is modified by nitric oxide (NO). Namely, parkin is *S*-nitrosylated in PD patients and an *in vivo* mouse model of PD, and *S*-nitrosylation shows inhibition of the E3 activity of

parkin (Chung *et al*, 2004; Kahle and Haass, 2004; Yao *et al*, 2004), which could contribute to the degenerative process in PD by impairing the ubiquitylation of parkin substrates. Moreover, Kalia *et al* (2004) showed that the bcl-2-associated athanogene 5 (BAG5) enhanced the death of dopaminergic neurons in an *in vivo* model of PD by inhibiting the E3 ligase activity of parkin. In addition, recent studies reported that phosphorylation of parkin causes a small but significant reduction of parkin auto-ubiquitylating activity (Yamamoto *et al*, 2004). More recently, it was reported that Nrdp1/FLRF RING-finger E3 ligase binds and ubiquitylates parkin, resulting in reduction of parkin activity, implying its involvement in the pathogenesis of PD (Zhong *et al*, 2005). Considered together, these results indicate that the apparent loss of parkin E3 ubiquitin ligase activity associated with the pathogenesis of PD (see the model displayed in Figure 6B) is in agreement with the ARJP-linked mutations that lead to loss of function of parkin, and that the functional loss of parkin activity is linked to the death of dopaminergic neurons. In addition, we reported herein the imbalance of tripartite interactions among parkin, 14-3-3η, and α-SN levels in the substantia nigra of sporadic PD, but it is still not clear how these alterations influence parkin activity in neural cells. Thus, parkin is an E3 ubiquitin ligase involved in the ubiquitylation of proteins, irrespective of its involvement of K48- or K63-linked ubiquitylation (Doss-Pepe *et al*, 2005; Lim *et al*, 2005), that are important in the survival of dopaminergic neurons in PD.

In the present study, we found that parkin E3 activity is regulated positively and negatively by α-SN and 14-3-3η, respectively, suggesting that derangements of this regulation may be responsible for ARJP. For instance, the activated parkin free from 14-3-3η may be labile, and thus sensitive to other stresses, such as *S*-nitrosylation, and inactivated secondarily in PD. This situation resembles the effect of *S*-nitrosylation, in which nitrosative stress leads to *S*-nitrosylation of WT parkin, which leads initially to a marked increase followed by a decrease in the E3 ligase–ubiquitin–proteasome degradative pathway (Yao *et al*, 2004). The initial increase in the activity of parkin's E3 ubiquitin ligase leads to autoubiquitylation of parkin and subsequent inhibition of its activity, which would impair ubiquitylation and clearance of parkin substrates. In turn, 14-3-3η may protect against impairment of parkin induced by various environmental stresses, including *S*-nitrosylation. It is also noteworthy that, although 14-3-3η acts as a negative regulator of parkin, it may play a positive role in maintaining a large pool of parkin by preventing its self-ubiquitylation in the brain. Finally, we assume that gradual reduction of parkin activity may be associated with the development of ARJP as well as sporadic PD.

Current evidence suggests that α-SN increases in response to various stresses (Sherer *et al*, 2002; Gomez-Santos *et al*, 2003). This finding is compatible with the results of recent studies that dopamine-dependent neurotoxicity (Tabrizi *et al*, 2000; Zhou *et al*, 2000; Junn and Mouradian, 2002) is mediated by the formation of protein complexes that contain α-SN and 14-3-3, which are selectively increased in the substantia nigra in PD (Xu *et al*, 2002). Further studies are needed to determine the levels of parkin, 14-3-3η, α-SN, and parkin and α-SN-14-3-3η complexes in the substantia nigra of the midbrain of patients with sporadic PD.

Here we suggest that α-SN and parkin function through the same pathway. Indeed, both proteins, if not all, are associated with presynaptic vesicles (Dawson and Dawson, 2003). So far, however, the physiological role of α-SN is largely unknown, though various roles including its involvement in synaptic plasticity have been suggested (Liu *et al*, 2004). We here provided the first evidence that α-SN acts as a positive regulator of parkin E3 activity. It is worth noting that disease-causing mutations of α-SN(A30P) and α-SN(A53T) could not activate the latent parkin–14-3-3η complex, and thus, these mutations may accelerate the development of PD by failing to activate parkin. Our results identified a functional link between these two familial PD-gene products, thus highlighting the existence of a novel regulatory mechanism that could help us further understand the pathogenesis of ARJP as well as sporadic PD. However, it must be stressed here that α-SN is the causative gene product of familial PD. It is noteworthy that α-SN is an aggregation-prone protein due to its natively unfolded protein nature. It is of note that the locus of *PARK4* is triplication of the α-*SN* gene (*PARK1*) (Singleton *et al*, 2003), indicating that overexpression of α-SN itself is toxic and induces dopaminergic neuronal death. Indeed, α-SN tends to self-aggregate, and this tendency, which is augmented in the α-SN(A30P) and α-SN(A53T) mutants (Conway *et al*, 2000) (see our model in Figure 6B), causes autosomal dominant PD (Narhi *et al*, 1999). Both WT and mutant α-SN form amyloid fibrils akin to those seen in LBs, as well as nonfibrillary oligomers termed protofibrils (Dawson and Dawson, 2003; Bossy-Wetzel *et al*, 2004). However, whether aggregation and fibrillary formation of α-SN- and PD-linked mutants play a role in neuronal dysfunction and death of neurons in PD are a matter of fierce debate. At this point of view, we emphasize that the feature of α-SN as an aggregation-prone protein is probably not linked directly to its role as a potent activator of parkin E3 in the pathogenesis of PD. Even if these two unique properties of α-SN account for the development of PD independently or synergistically, however, it is clear that their mechanistic actions differ as illustrated in Figure 6B.

Materials and methods

Immunological analysis

For immunoprecipitation analysis of endogenous proteins in the brains of adult mouse and human, these brains were homogenized in three volumes of ice-cold lysis buffer (20 mM HEPES (pH 7.9) buffer containing 0.2% NP-40, 1 mM dithiothreitol (DTT) and protease inhibitor cocktail (Sigma, Chemical Co., St Louis, MO)). The tissue homogenate was centrifuged at 20 000 *g* at 4°C for 20 min. The supernatant (2 mg protein) was used for immunoprecipitation with one of the following antibodies: anti-polyclonal parkin (Cell Signaling Technology, Beverly, MA) and anti-14-3-3η antibodies (Immuno-Biological Lab. Co., Gunma) or control IgG (700 ng). The resulting immunoprecipitates were resolved in 30 μl of the sodium dodecyl sulfate–polyacrylamide gel electrophoresis (SDS–PAGE) sample buffer, and one-third of the samples (10 μl) were subjected to SDS–PAGE, followed by Western blotting with anti-14-3-3 (Santa Cruz Biotechnology, Santa Cruz, CA), anti-14-3-3β, 14-3-3γ, 14-3-3ε, 14-3-3η, and 14-3-3τ (Immuno-Biological Lab. Co., Ltd, Japan) and anti-monoclonal parkin (1A1) antibodies (Shimura *et al*, 1999). In all, 10 μg of the supernatant (lysate) was used as input (1.5%).

For immunoprecipitation analysis of the cell culture system, HEK293 cells were transfected with the respective plasmids. After 48 h, the cells were washed with ice-cold PBS (in mM, 10 Na_2PO_4, 2 KH_2PO_4, 137 NaCl, and 2.7 KCl), pH 7.4, and harvested in the lysis buffer (600 μl). The lysate was then rotated at 4°C for 1 h, followed by centrifugation at 20 000 *g* for 10 min. The supernatant (200 μl) was then combined with 50 μl protein G-Sepharose (Amersham Life

Science, Buckinghamshire, UK), pre-incubated with anti-Myc (Santa Cruz Biotechnology, Santa Cruz), V5 (Invitrogen), and HA (Santa Cruz Biotechnology) antibodies or anti-FL antibody beads (Sigma) for 3 h. The protein G-Sepharose or FL-beads were precipitated and the pellets were extensively washed using the lysis buffer containing 500 mM NaCl. The precipitates were used for Western blot analysis using anti-parkin, Myc, FL, HA, V5, 14-3-3, and α-SN (BD Transduction Lab.) antibodies, as mentioned above. A volume of 5 μl of the supernatant was used as input (7.5%).

In vitro autoubiquitylation assay

Recombinant GST-14-3-3η was produced in *Escherichia coli*. Untagged 14-3-3η was produced from GST-14-3-3η by digestion with PreScission Protease (Amersham Bioscience). Recombinant His-parkin and E1 were produced from baculovirus-infected HiFive insect cells. Reactions were performed for 3 h at 37°C in 50 μl of assay mixture containing 40 mM Tris–HCl buffer (pH 7.5), 5 mM $MgCl_2$, 2 mM ATP, 2 mM DTT, 15 μg ubiquitin (Sigma), 200 ng of E1, and 600 ng of E2 (UbcH7) (Affiniti-Research, Exeter, Devon, UK) in the presence or absence of GST-14-3-3η or 14-3-3η. After incubation, the reaction was terminated by the addition of the sample buffer for SDS–PAGE (17 μl), and aliquots (15 μl) were subjected to SDS–PAGE followed by Western blotting with anti-parkin antibody.

In vivo ubiquitylation assay

HEK293 cells were transfected for 48 h with pcDNA3.1 expression plasmids, in which FL-tagged parkin or FL-parkin mutants, α-SN or α-SN mutants, 14-3-3η, V5-synphilin-1, and HA-ubiquitin cDNAs were ligated. MG132 (50 μM) was added for 20 min, prior to harvesting of the cells. Then, the cells were washed with cold PBS and lysed by 50 mM Tris–HCl buffer (pH 8.0), containing 150 mM NaCl, 1% Nonidet-P40, 1% deoxycolate, 0.1% SDS, 5 mM ethylenediaminetetraacetic acid, and protease inhibitor cocktail. Preparation of the cell lysate, immunoprecipitation, and Western blot analyses were essentially the same for the immunological analysis as described above. In all experiments, the cell lysates (10 μg, 7.5% input) were used for Western blotting as controls to check the expression levels.

For the method sections of 'Cell culture and transfection', 'Plasmids', and 'Surface plasmon resonance (SPR) analysis', see Supplementary data.

Supplementary data

Supplementary data are available at *The EMBO Journal* Online.

Acknowledgements

We thank Y Goto for providing the 14-3-3σ, β, and ζ expression plasmids, and T Ichimura for the valuable discussion. This work was supported in part by Grants-in-Aid from the Ministry of Education, Culture, Sports, Science and Technology of Japan.

References

Aitken A (2002) Functional specificity in 14-3-3 isoform interactions through dimer formation and phosphorylation. Chromosome location of mammalian isoforms and variants. *Plant Mol Biol* **50:** 993–1010

Aitken A, Baxter H, Dubois T, Clokie S, Mackie S, Mitchell K, Peden A, Zemlickova E (2002) Specificity of 14-3-3 isoform dimer interactions and phosphorylation. *Biochem Soc Trans* **30:** 351–360

Baxter HC, Liu WG, Forster JL, Aitken A, Fraser JR (2002) Immunolocalisation of 14-3-3 isoforms in normal and scrapie-infected murine brain. *Neuroscience* **109:** 5–14

Berg D, Holzmann C, Riess O (2003) 14-3-3 proteins in the nervous system. *Nat Rev Neurosci* **4:** 752–762

Bossy-Wetzel E, Schwarzenbacher R, Lipton SA (2004) Molecular pathways to neurodegeneration. *Nat Med* **10** (Suppl S2): S2–S9

Bridges D, Moorhead GB (2004) 14-3-3 proteins: a number of functions for a numbered protein. *Sci STKE* **2004:** re10

Chung KK, Thomas B, Li X, Pletnikova O, Troncoso JC, Marsh L, Dawson VL, Dawson TM (2004) *S*-nitrosylation of parkin regulates ubiquitination and compromises parkin's protective function. *Science* **304:** 1328–1331

Chung KK, Zhang Y, Lim KL, Tanaka Y, Huang H, Gao J, Ross CA, Dawson VL, Dawson TM (2001) Parkin ubiquitinates the α-synuclein-interacting protein, synphilin-1: implications for Lewy-body formation in Parkinson disease. *Nat Med* **7:** 1144–1150

Conway KA, Lee SJ, Rochet JC, Ding TT, Williamson RE, Lansbury Jr PT (2000) Acceleration of oligomerization, not fibrillization, is a shared property of both α-synuclein mutations linked to early-onset Parkinson's disease: implications for pathogenesis and therapy. *Proc Natl Acad Sci USA* **97:** 571–576

Dawson TM, Dawson VL (2003) Molecular pathways of neurodegeneration in Parkinson's disease. *Science* **302:** 819–822

Doss-Pepe EW, Chen L, Madura K (2005) α-Synuclein and parkin contribute to the assembly of ubiquitin lysine 63-linked multiubiquitin chains. *J Biol Chem* **280:** 16619–16624

Forno LS (1996) Neuropathology of Parkinson's disease. *J Neuropathol Exp Neurol* **55:** 259–272

Fujiwara H, Hasegawa M, Dohmae N, Kawashima A, Masliah E, Goldberg MS, Shen J, Takio K, Iwatsubo T (2002) α-Synuclein is phosphorylated in synucleinopathy lesions. *Nat Cell Biol* **4:** 160–164

Gomez-Santos C, Ferrer I, Santidrian AF, Barrachina M, Gil J, Ambrosio S (2003) Dopamine induces autophagic cell death and α-synuclein increase in human neuroblastoma SH-SY5Y cells. *J Neurosci Res* **73:** 341–350

Hallberg B (2002) Exoenzyme S binds its cofactor 14-3-3 through a non-phosphorylated motif. *Biochem Soc Trans* **30:** 401–405

Hirai Y, Fujita SC, Iwatsubo T, Hasegawa M (2004) Phosphorylated α-synuclein in normal mouse brain. *FEBS Lett* **572:** 227–232

Imai Y, Soda M, Inoue H, Hattori N, Mizuno Y, Takahashi R (2001) An unfolded putative transmembrane polypeptide, which can lead to endoplasmic reticulum stress, is a substrate of Parkin. *Cell* **105:** 891–902

Junn E, Mouradian MM (2002) Human α-synuclein over-expression increases intracellular reactive oxygen species levels and susceptibility to dopamine. *Neurosci Lett* **320:** 146–150

Kahle PJ, Haass C (2004) How does parkin ligate ubiquitin to Parkinson's disease? *EMBO Rep* **5:** 681–685

Kalia SK, Lee S, Smith PD, Liu L, Crocker SJ, Thorarinsdottir TE, Glover JR, Fon EA, Park DS, Lozano AM (2004) BAG5 inhibits parkin and enhances dopaminergic neuron degeneration. *Neuron* **44:** 931–945

Kawakami T, Chiba T, Suzuki T, Iwai K, Yamanaka K, Minato N, Suzuki H, Shimbara N, Hidaka Y, Osaka F, Omata M, Tanaka K (2001) NEDD8 recruits E2-ubiquitin to SCF E3 ligase. *EMBO J* **20:** 4003–4012

Kawamoto Y, Akiguchi I, Nakamura S, Honjyo Y, Shibasaki H, Budka H (2002) 14-3-3 proteins in Lewy bodies in Parkinson disease and diffuse Lewy body disease brains. *J Neuropathol Exp Neurol* **61:** 245–253

Kruger R, Kuhn W, Muller T, Woitalla D, Graeber M, Kosel S, Przuntek H, Epplen JT, Schols L, Riess O (1998) A30P mutation in the gene encoding α-synuclein in Parkinson's disease. *Nat Genet* **18:** 106–108

Lim KL, Chew KC, Tan JM, Wang C, Chung KK, Zhang Y, Tanaka Y, Smith W, Engelender S, Ross CA, Dawson VL, Dawson TM (2005) Parkin mediates nonclassical, proteasomal-independent ubiquitination of synphilin-1: implications for Lewy body formation. *J Neurosci* **25:** 2002–2009

Liu S, Ninan I, Antonova I, Battaglia F, Trinchese F, Narasanna A, Kolodilov N, Dauer W, Hawkins RD, Arancio O (2004) Synuclein produces a long-lasting increase in neurotransmitter release. *EMBO J* **23:** 4506–4516

Mackintosh C (2004) Dynamic interactions between 14-3-3 proteins and phosphoproteins regulate diverse cellular processes. *Biochem J* **381:** 329–342

Martin H, Rostas J, Patel Y, Aitken A (1994) Subcellular localisation of 14-3-3 isoforms in rat brain using specific antibodies. *J Neurochem* **63:** 2259–2265

McNaught KS, Olanow CW (2003) Proteolytic stress: a unifying concept for the etiopathogenesis of Parkinson's disease. *Ann Neurol* **53** (Suppl 3): S73–S84

Narhi L, Wood SJ, Steavenson S, Jiang Y, Wu GM, Anafi D, Kaufman SA, Martin F, Sitney K, Denis P, Louis JC, Wypych J, Biere AL, Citron M. (1999) Both familial Parkinson's disease mutations accelerate α-synuclein aggregation. *J Biol Chem* **274:** 9843–9846

Ostrerova N, Petrucelli L, Farrer M, Mehta N, Choi P, Hardy J, Wolozin B (1999) α-Synuclein shares physical and functional homology with 14-3-3 proteins. *J Neurosci* **19:** 5782–5791

Polymeropoulos MH, Lavedan C, Leroy E, Ide SE, Dehejia A, Dutra A, Pike B, Root H, Rubenstein J, Boyer R, Stenroos ES, Chandrasekharappa S, Athanassiadou A, Papapetropoulos T, Johnson WG, Lazzarini AM, Duvoisin RC, Di Iorio G, Golbe LI, Nussbaum RL (1997) Mutation in the α-synuclein gene identified in families with Parkinson's disease. *Science* **276:** 2045–2047

Roberts MR, de Bruxelles GL (2002) Plant 14-3-3 protein families: evidence for isoform-specific functions? *Biochem Soc Trans* **30:** 373–378

Sherer TB, Betarbet R, Stout AK, Lund S, Baptista M, Panov AV, Cookson MR, Greenamyre JT (2002) An *in vitro* model of Parkinson's disease: linking mitochondrial impairment to altered α-synuclein metabolism and oxidative damage. *J Neurosci* **22:** 7006–7015

Shimura H, Hattori N, Kubo S, Mizuno Y, Asakawa S, Minoshima S, Shimizu N, Iwai K, Chiba T, Tanaka K, Suzuki T (2000) Familial Parkinson disease gene product, parkin, is a ubiquitin-protein ligase. *Nat Genet* **25:** 302–305

Shimura H, Hattori N, Kubo S, Yoshikawa M, Kitada T, Matsumine H, Asakawa S, Minoshima S, Yamamura Y, Shimizu N, Mizuno Y (1999) Immunohistochemical and subcellular localization of Parkin protein: absence of protein in autosomal recessive juvenile parkinsonism patients. *Ann Neurol* **45:** 668–672

Singleton AB, Farrer M, Johnson J, Singleton A, Hague S, Kachergus J, Hulihan M, Peuralinna T, Dutra A, Nussbaum R, Lincoln S, Crawley A, Hanson M, Maraganore D, Adler C, Cookson MR, Muenter M, Baptista M, Miller D, Blancato J, Hardy J, Gwinn-Hardy K (2003) α-Synuclein locus triplication causes Parkinson's disease. *Science* **302:** 841

Sribar J, Sherman NE, Prijatelj P, Faure G, Gubensek F, Fox JW, Aitken A, Pungercar J, Krizaj I (2003) The neurotoxic phospholipase A2 associates, through a non-phosphorylated binding motif, with 14-3-3 protein γ and ε isoforms. *Biochem Biophys Res Commun* **302:** 691–696

Tabrizi SJ, Orth M, Wilkinson JM, Taanman JW, Warner TT, Cooper JM, Schapira AH (2000) Expression of mutant α-synuclein causes increased susceptibility to dopamine toxicity. *Hum Mol Genet* **9:** 2683–2689

Ubl A, Berg D, Holzmann C, Kruger R, Berger K, Arzberger T, Bornemann A, Riess O (2002) 14-3-3 protein is a component of Lewy bodies in Parkinson's disease-mutation analysis and association studies of 14-3-3η. *Brain Res Mol Brain Res* **108:** 33–39

Vila M, Przedborski S (2004) Genetic clues to the pathogenesis of Parkinson's disease. *Nat Med* **10** (Suppl): S58–S62

Xu J, Kao SY, Lee FJ, Song W, Jin LW, Yankner BA (2002) Dopamine-dependent neurotoxicity of α-synuclein: a mechanism for selective neurodegeneration in Parkinson disease. *Nat Med* **8:** 600–606

Yaffe MB, Rittinger K, Volinia S, Caron PR, Aitken A, Leffers H, Gamblin SJ, Smerdon SJ, Cantley LC (1997) The structural basis for 14-3-3:phosphopeptide binding specificity. *Cell* **91:** 961–971

Yamamoto A, Friedlein A, Imai Y, Takahashi R, Kahle PJ, Haass C (2004) Parkin phosphorylation and modulation of its E3 ubiquitin ligase activity. *J Biol Chem* **280:** 3390–3399

Yao D, Gu Z, Nakamura T, Shi ZQ, Ma Y, Gaston B, Palmer LA, Rockenstein EM, Zhang Z, Masliah E, Uehara T, Lipton SA (2004) Nitrosative stress linked to sporadic Parkinson's disease: S-nitrosylation of parkin regulates its E3 ubiquitin ligase activity. *Proc Natl Acad Sci USA* **101:** 10810–10814

Zhong L, Tan Y, Zhou A, Yu Q, Zhou J (2005) RING finger ubiquitin-protein isopeptide ligase Nrdp1/FLRF regulates parkin stability and activity. *J Biol Chem* **280:** 9425–9430

Zhou W, Hurlbert MS, Schaack J, Prasad KN, Freed CR (2000) Overexpression of human α-synuclein causes dopamine neuron death in rat primary culture and immortalized mesencephalon-derived cells. *Brain Res* **866:** 33–43

THE JOURNAL OF BIOLOGICAL CHEMISTRY VOL. 281, NO. 6, pp. 3204–3209, February 10, 2006

Diverse Effects of Pathogenic Mutations of Parkin That Catalyze Multiple Monoubiquitylation *in Vitro*[*] [S]

Received for publication, September 21, 2005, and in revised form, November 29, 2005 Published, JBC Papers in Press, December 8, 2005, DOI 10.1074/jbc.M510393200

Noriyuki Matsuda[‡], Toshiaki Kitami[§], Toshiaki Suzuki[‡], Yoshikuni Mizuno[§], Nobutaka Hattori[§], and Keiji Tanaka[‡1]

From the [‡]Laboratory of Frontier Science, Tokyo Metropolitan Institute of Medical Science, Bunkyo-ku, Tokyo 113-8613 and the [§]Department of Neurology, Juntendo University School of Medicine, 2-1-1 Hongo, Bunkyo-ku, Tokyo 113-0033, Japan

Mutational dysfunction of *PARKIN* gene, which encodes a double RING finger protein and has ubiquitin ligase E3 activity, is the major cause of autosomal recessive juvenile Parkinsonism. Although many studies explored the functions of Parkin, its biochemical character is poorly understood. To address this issue, we established an E3 assay system using maltose-binding protein-fused Parkin purified from *Escherichia coli*. Using this recombinant Parkin, we found that not the front but the rear RING finger motif is responsible for the E3 activity of Parkin, and it catalyzes multiple monoubiquitylation. Intriguingly, for autosomal recessive juvenile Parkinsonism-causing mutations of Parkin, whereas there was loss of E3 activity in the rear RING domain, other pathogenic mutants still exhibited E3 activity equivalent to that of the wild-type Parkin. The evidence presented allows us to reconsider the function of Parkin-catalyzed ubiquitylation and to conclude that autosomal recessive juvenile Parkinsonism is not solely attributable to catalytic impairment of the E3 activity of Parkin.

Recessive mutations in the human *PARKIN* gene are the most frequent cause of autosomal recessive juvenile parkinsonism, the common form of familial Parkinson disease (PD).[2] It has been shown that almost 50% of patients with familial autosomal recessive juvenile parkinsonism carry a series of exon rearrangements or point mutations in *PARKIN*. Moreover, recent findings of the haploinsufficiency of *parkin* and *S*-nitrosylation also imply its association in sporadic PD (1). The causal gene *PARKIN* encodes a double RING finger protein with ubiquitin ligase (E3) activity (2–5) and interestingly, missense mutations in the double RING finger motif resulted in an earlier onset of the disease than mutations in other function-unknown regions (6). To date, numerous biochemical studies have been performed to understand how mutations in Parkin lead to its dysfunction and to pathogenic outcome. However, because the biochemical characterization of E3 activity of Parkin has been difficult, it is still controversial whether the disease-relevant Parkin mutants lose their E3 activity or not. For example, one group of investigators implied that Parkin harboring K161N mutation loses its E3 activity (7), whereas another group suggested the same mutation dose not impair E3 activity (8). In the case of other PD mutations, the situation is even more complex (see supplemental Table 1). Thus, the mode of Parkin-catalyzed ubiquitylation remains poorly understood to date.

Little is known about the reconstituted ubiquitylating experiment using recombinant Parkin. Almost all of the biochemical analyses reported so far have been performed using *in vitro* translated Parkin or immunoprecipitated Parkin. However, it is difficult to avoid trace contaminants of other proteins that could physically interact with Parkin. Indeed it has been reported that Parkin interacts with other E3s such as CHIP (9) and Nrdp1/FLRF (10), and thus the results of experiments using immunoprecipitated or *in vitro* translated Parkin require careful interpretation. To study the E3 activity of intrinsic Parkin, a biochemical approach using bacterially expressed recombinant Parkin that is free from other contaminating E3 enzyme(s) is obviously required. We thus attempted to reconstitute a sensitive E3 assay system using Parkin purified from *Escherichia coli*.

EXPERIMENTAL PROCEDURES

Purification of Recombinant Proteins—To express Parkin in *E. coli*, it was important to use a modified *E. coli* strain BL21(DE3) codon-plus (RIL) strain (Stratagene, La Jolla, CA), because Parkin possesses many rare codons for *E. coli* that might cause low expression and/or amino acid misincorporation. For example, Parkin contains eight AGA codons that lead to mistranslation of lysine for arginine in *E. coli* (11). pMAL-p2T, in which the thrombin recognition site was inserted into pMALp2 (New England BioLabs, Beverly, MA), was prepared to purify maltose-binding protein (MBP)-LVPRGS-Parkin. Parkin cDNAs of wild type and various mutants/deletions were subcloned into BamHI site of pMAL-p2 and pMAL-p2T. All mutants/deletions were generated by PCR-mediated site-directed mutagenesis (details of the plasmid construction processes can be provided upon request). All recombinant fusion proteins were purified from bacterial lysate applying the method advocated by the supplier (New England BioLabs) using a column buffer containing 20 mM Tris-HCl, pH 7.5, 200 mM NaCl, 1 mM dithiothreitol, and 100 μM $ZnSO_4$. The eluted fraction containing 10 mM maltose was not dialyzed because Parkin tends to lose its E3 activity during dialysis. Instead, it was subjected to the ubiquitylation assay directly. We attempted to purify sole IBR-RING2 region of Parkin also by splitting MBP-IBR-RING2 (see "Results"). Specifically, we added E2, various detergents and stabilizers during the cleavage process expecting that they solubilize and/or stabilize free IBR-RING2 in solution. Even in all the above experimental conditions, however, we could not obtain soluble-free IBR-RING2 (data not shown). Six histidine-tagged proteins such as Uev1/Ubc13 were purified by the conventional method and dialyzed by a buffer containing 20 mM Tris-HCl, pH 8.0, 200 mM NaCl and 1 mM dithiothreitol. Glycerol of 6% was added as a stabilizer for preservation of recombinant MBP-Parkin and E2 proteins at −80 °C.

In Vitro Ubiquitylation Assay—The *in vitro* ubiquitylation assay was performed as described previously (12–14). Briefly, the purified MBP-Parkin (20 μg of MBP-Parkin/ml) was incubated in a reaction buffer (50

* This work was supported by grants-in-aid from the Ministry of Education, Culture, Sports, Science and Technology of Japan (to K. T.). The costs of publication of this article were defrayed in part by the payment of page charges. This article must therefore be hereby marked "*advertisement*" in accordance with 18 U.S.C. Section 1734 solely to indicate this fact.

[S] The on-line version of this article (available at http://www.jbc.org) contains supplemental Table 1 and Fig. 1.

[1] To whom correspondence should be addressed. Tel. and Fax: +81-3-3823-2237; E-mail: tanakak@rinshoken.or.jp.

[2] The abbreviations used are: PD, Parkinson disease; E1, ubiquitin-activating enzyme; E2, ubiquitin-conjugating enzyme; E3, ubiquitin ligase; GST, glutathione *S*-transferase; MBP, maltose-binding protein.

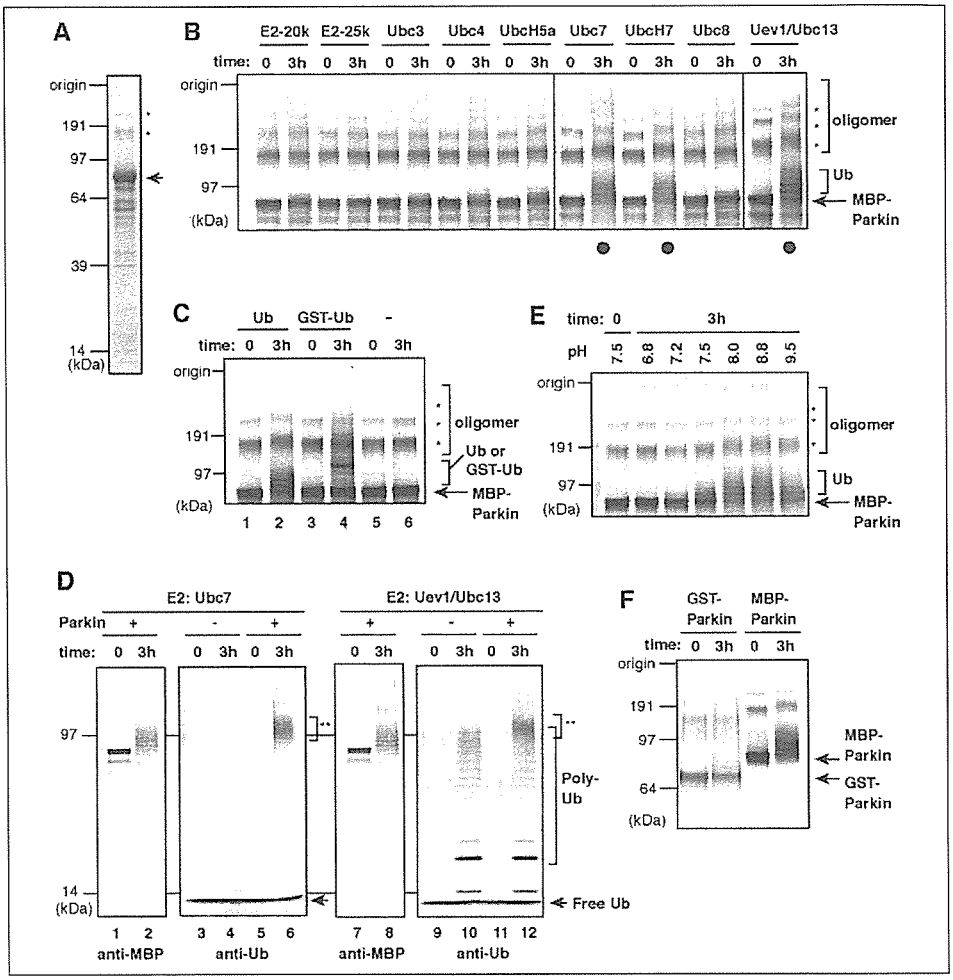

FIGURE 1. ***In vitro* ubiquitylation assay using Parkin derived from *E. coli*.** *A*, purified MBP-Parkin was visualized by CBB staining. The *arrow* indicates MBP-Parkin, and the *asterisks* indicate oligomerization bands. *B*, MBP-Parkin catalyzes autoubiquitylation in cooperation with Ubc7, UbcH7, and Uev1-Ubc13 (*solid circles*). MBP-Parkin was subjected to *in vitro* ubiquitylation assay and to immunoblotting with anti-MBP antibody. *Ub*, ladders derived from autoubiquitylation, *, oligomerization bands. *C*, confirmation of autoubiquitylation of MBP-Parkin. To demonstrate that the slower migrating ladders are because of autoubiquitylation, a reconstitution assay was repeated in the absence (−) or presence of ubiquitin (*Ub*) or GST-ubiquitin (*GST-Ub*). *D*, the high molecular weight forms of MBP-Parkin are recognized by anti-ubiquitin antibody. *Double asterisks* indicate the signal derived from MBP-Parkin autoubiquitylation. The *arrow* indicates free ubiquitin. *E*, Parkin prefers weak alkaline conditions to exert its E3 activity. *F*, GST-Parkin rarely exhibits E3 activity. Bacterial recombinant GST- and MBP-Parkin were concurrently subjected to ubiquitylation assay. Ubc7 was used as E2 in *C*, *E*, and *F*. Anti-MBP antibody was used in *B*, *C*, and *E*, and anti-Parkin antibody was used in *F*.

mM Tris-HCl, pH 8.8, 2 mM dithiothreitol, 5 mM $MgCl_2$, and 4 mM ATP) with 50 μg of ubiquitin/ml (Sigma), 1.6 μg of recombinant mouse E1/ml and 20 μg of purified E2 or 100 μg of various E2-expressing *E. coli* lysate/ml at 32 °C for 2 h and subjected to immunoblotting with anti-MBP antibody (New England BioLabs), anti-parkin (1A1) antibody (15), or anti-ubiquitin antibody (DakoCytomation, Carpinteria, CA). In some cases, GST-ubiquitin or methylated ubiquitin (BostonBiochem, Cambridge, MA) was used instead of native ubiquitin. The subsequent thrombin cleavage was performed by incubation on ice for 3 h in the presence of thrombin and 2 mM $CaCl_2$.

RESULTS

Autoubiquitylation by MBP-Parkin Fusion Protein—In 2001, Rankin *et al.* (16) reported that glutathione *S*-transferase (GST)-tagged Parkin purified from *E. coli* possesses E3 activity. However, we found that the E3 activity of this GST-Parkin is very weak (Fig. 1*F*), and thus there is a need for a more sensitive E3 assay system for bacterially expressed recombinant Parkin. During studies of other RING finger proteins, we recognized the superiority of the MBP-tag relative to GST-tag in purifying RING finger proteins that retain their E3 activities (12, 13, 17, 18) and hence decided to use MBP-Parkin. MBP-Parkin was purified using a modified *E. coli* strain BL21(DE3) codon-plus-RIL (Fig. 1*A*) and then incubated with ATP, ubiquitin, E1, and one of the E2 enzymes indicated in Fig. 1*B*, and we subjected it to immunoblotting with anti-MBP antibody. High molecular mass ladders derived from autoubiquitylation (see below) were observed when MBP-Parkin was incubated with Ubc7, UbcH7, and Uev1-Ubc13 (Fig. 1*B*, highlighted by the *solid circles*). Note that the slower migrating bands of more than 160 kDa observed even at reaction time zero (Fig. 1*B*, *asterisks*) or without ubiquitin (Fig. 1, *A* and *C*, *asterisks*) are derived from MBP-Parkin oligomerization. To test whether the modification acquired by MBP-Parkin is due to ubiquitylation, the same reaction products were subjected to immunoblotting with anti-ubiquitin antibody. When Ubc7 was used as E2 (Fig. 1*D*, *lanes 1–6*), only modified MBP-Parkin was detected by anti-ubiquitin antibody (*lane 6*, *double asterisks*), indicating that the modification acquired by MBP-Parkin was indeed autoubiquitylation. When Uev1-Ubc13 was used, a polyubiquitylation signal was observed even in the absence of MBP-Parkin (Fig. 1*D*, *lanes 9* and *10*), because Uev1-Ubc13 complex itself can catalyze polyubiquitin chain formation (19). Also in this case, modified MBP-Parkin reacted with anti-ubiquitin antibody, confirming the above conclusion (see Fig. 1*D*, *double asterisks* in *lane 12*; note that the difference between *lanes 10* and *12* corresponds to the autoubiquitylation signal of MBP-Parkin). Moreover, the replacement of ubiquitin with GST-ubiquitin retarded the mobility of these ladders (Fig. 1*C*, *lanes 3* and *4*), and the exclusion of ubiquitin completely quenched such ladders (Fig. 1*C*, *lanes 5* and *6*). Based on these results, we concluded that MBP-Parkin catalyzes autoubiquitylation in cooperation with Ubc7, UbcH7, and Uev1-Ubc13. Interestingly, autoubiquitylation became evident when the pH of the reaction buffer was increased to 8.0 and 8.8, indicating that Parkin prefers weak alkaline conditions to exhibit its E3 activity *in vitro* (Fig. 1*E*). Because MBP-Parkin possesses stronger E3

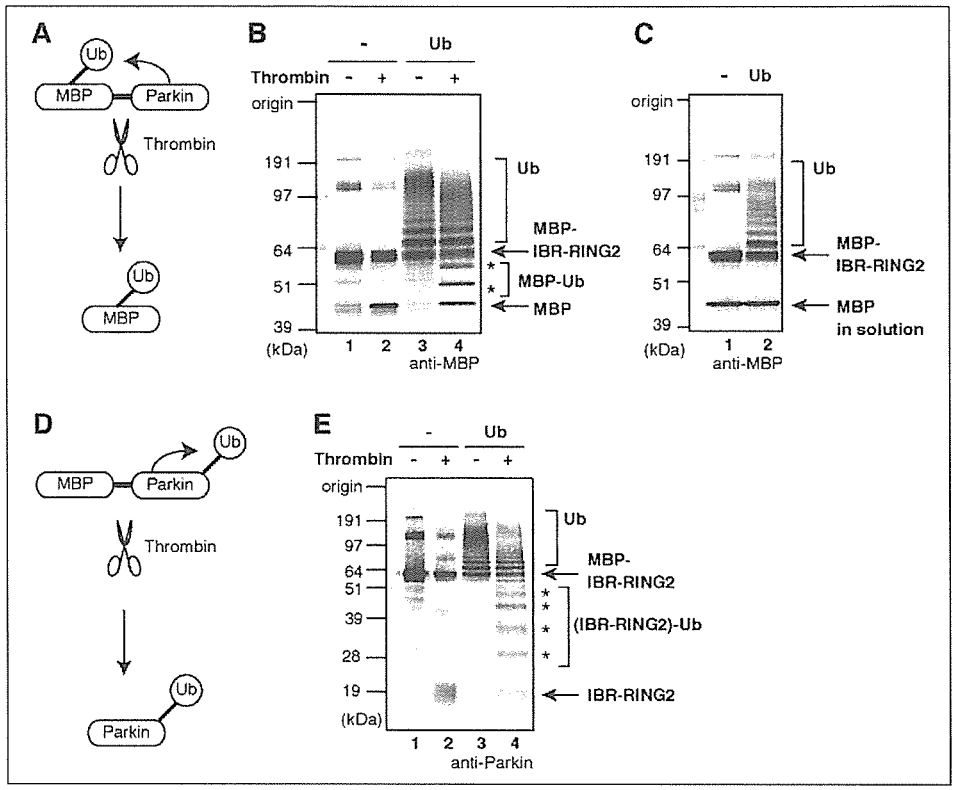

FIGURE 2. **In-frame-fused MBP can be a good pseudosubstrate of Parkin.** *A*, a schematic diagram of Parkin catalyzed ubiquitylation of MBP. If the MBP portion is ubiquitylated, a change in its mobility would be recognized by immunoblotting after cleavage. *B*, the MBP-(IBR-RING2) fused protein (see Fig. 4) was subjected to *in vitro* ubiquitylation, subsequent cleavage into MBP moiety, and immunoblotting with anti-MBP antibody. The MBP portion of IBR-RING2 was ubiquitylated (*asterisks*). *C*, MBP can be ubiquitylated only when it is in the physical vicinity of Parkin. Note that free MBP in solution was not ubiquitylated. *D*, a schematic diagram of Parkin-catalyzed autoubiquitylation. *E*, IBR-RING2 portion is also ubiquitylated. *Asterisks* in *lane 4* show the ubiquitylated IBR-RING2 moiety (compare *lane 4* with *2*). Ubc7 was used as E2 in these experiments.

activity than GST-Parkin, as shown in Fig. 1*F*, we used MBP-Parkin in the following experiments.

Fused MBP Is a Good Pseudo-substrate to Monitor E3 Activity of Parkin—We next determined whether the MBP portion or Parkin portion (or both) is ubiquitylated. To check this, we purified MBP-LVPRGS-Parkin, in which a thrombin-digestion sequence is inserted between MBP and Parkin. As depicted in Fig. 2*A*, if the MBP moiety is ubiquitylated, its molecular weight would increase by ubiquitylation and subsequent digestion, but if not ubiquitylated, its molecular weight would remain unchanged. First we tried to split MBP-LVPRGS-Parkin by thrombin; however, this recombinant protein was hardly digested for some unknown reason (data not shown). We next fused the C-terminal IBR-RING2 region of Parkin to MBP-LVPRGS (hereafter dubbed IBR-RING2, see Fig. 4*A*), and this construct was cleaved moderately (Fig. 2*B*, *lanes 1* and *2*). When IBR-RING2 was subjected to an ubiquitylation assay and subsequently separated into MBP and IBR-RING2 portions by thrombin digestion, the molecular weight of MBP moiety was clearly increased (see the *asterisks* in Fig. 2*B*, *lanes 3* and *4*), meaning that the MBP portion is ubiquitylated. Does this result mean that bacterial MBP protein is the substrate for Parkin? The answer is no. When sole MBP protein was incubated with IBR-RING2, this free MBP was not ubiquitylated at all, even though IBR-RING2 was autoubiquitylated as described (Fig. 2, compare *C* with *B*). This result indicates that the IBR-RING2 region of Parkin ubiquitylates fused-MBP, but not unbound MBP, and strongly suggests that Parkin recognizes MBP as a substrate not because of its amino acid sequence but because of its physical vicinity to Parkin. As depicted in Fig. 2*D*, when the same experiment was repeated using an anti-Parkin antibody, the molecular weight of the IBR-RING2 moiety was also increased meaning that both MBP and IBR-RING2 portions were ubiquitylated (Fig. 2*E*). Although many putative substrates of Parkin have been reported, the lack of a good *in vitro* substrate makes any biochemical study difficult. Our study revealed that fused MBP could be a good pseudo-substrate to monitor the E3 activity of Parkin.

Parkin by Itself Catalyzes Multiple Monoubiquitylation—The Uev1-Ubc13 heterodimer is an E2 involved in the formation of Lys-63-linked polyubiquitylation (19). We confirmed that our Uev1-Ubc13 complex is functional (Fig. 1*D* and supplemental Fig. 1*A*). Motivated by the findings that Parkin catalyzes Lys-63-linked polyubiquitylation (20, 21) and Parkin cooperates with Uev1-Ubc13 in our assay (Fig. 1*B*), we investigated the mode of Parkin-catalyzed ubiquitylation. Parkin could either catalyze multiple monoubiquitylation, Lys-48-linked polyubiquitylation, or Lys-63-linked polyubiquitylation. Lys-48-linked polyubiquitylation has been studied most and it essentially directs the substrate to degradation by the proteasome. In contrast, the Lys-63-linked polyubiquitylation and monoubiquitylation serve as a signal other than proteasomal-proteolysis (22–24). We first used methylated ubiquitin (hereafter referred to as Met-Ub) in which all lysine residues are blocked by methylation and is incapable of polyubiquitylation. If Parkin catalyzes polyubiquitylation, the use of Met-Ub would shorten the ladder of ubiquitylation but if not, the ubiquitylation pattern would remain unchanged. Unexpectedly, the use of Met-Ub and Uev1-Ubc13 did not change the ubiquitylation pattern, indicating that Parkin catalyzes multiple monoubiquitylation *in vitro* (Fig. 3*A*). The same result was observed when Ubc7 was used as E2 (Fig. 3*B*), and these results were more evident when IBR-RING2 (Fig. 4*A*) was utilized (Fig. 3, *C* and *D*). Repeated experiments using lysine-less ubiquitin, in which all lysine residues were changed to arginine, showed it cannot form a polyubiquitin chain, again confirmed the consequence (Fig. 3*E*). It is noteworthy that sole Ubc13 itself assisted autoubiquitylation of Parkin as well as the Uev1-Ubc13 complex (supplemental Fig. 1*B*), again supporting this conclusion. These results allowed us to conclude that the mode of ubiquitylation catalyzed by intrinsic Parkin *in vitro* is multiple monoubiquitylation rather than polyubiquitylation (see "Discussion").

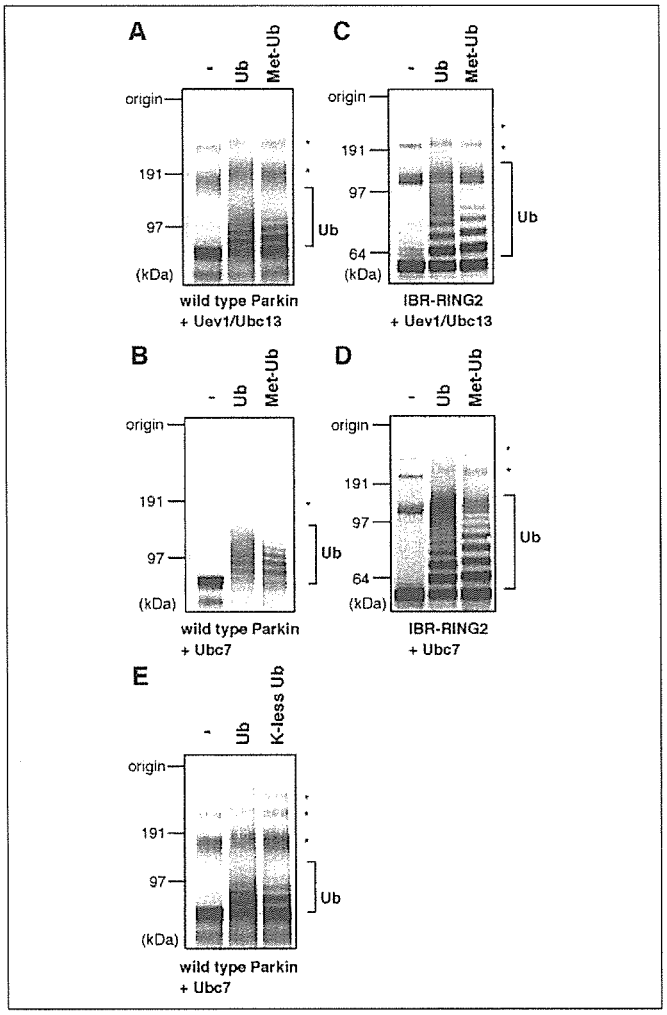

FIGURE 3. **Parkin catalyzes multiple monoubiquitylation.** *A* and *B*, *in vitro* ubiquitylation assay was performed in the absence (−) or presence of ubiquitin (*Ub*) or methylated-ubiquitin (*Met-Ub*; cannot form polyubiquitylation chain). Uev1-Ubc13 was used as E2 in *A* and Ubc7 in *B*. Almost identical ubiquitylation patterns were observed in Ub and Met-Ub, indicating that Parkin catalyzes multiple monoubiquitylation. *C* and *D*, the result was more evident when IBR-RING2 (see Fig. 4) was utilized. Uev1-Ubc13 was used as E2 in *C* and Ubc7 in *D*. *E*, the same experiment was performed using lysine-less ubiquitin. *Ub*, autoubiquitylation; *, oligomerization bands. Anti-MBP antibody was used in all experiments.

Mode of E3 Activity of Parkin with Pathogenic Missense Mutations—At present, dozens of disease-relevant mutations of Parkin have been reported, and the primary cause of autosomal recessive juvenile parkinsonism is assumed to be impairment of the E3 activity of Parkin by such mutations. However, it is still contentious whether Parkin with PD-causing mutation loses its E3 activity or not (see supplemental Table 1), primarily because of the absence of a sensitive E3-activity assay system using recombinant Parkin. To settle this problem, we examined the E3 activity of MBP-Parkin harboring various mutations and deletions. Three in-frame exonic deletions and 19 PD-linked mutations distributed throughout Parkin were selected (Fig. 4*A*). In addition, two Parkin species, one lacks its Ubl domain (ΔUbl) and the other possesses only C-terminally IBR-RING2 domain (IBR-RING2), were also generated. When these MBP-Parkin mutants were incubated with Ubc7 as E2, only mutations neighboring the second RING finger motif (Fig. 4*A*, *solid circles*) abolished the E3 activity completely (Fig. 4*B*). A nonsense mutation lacking the rear RING finger motif had no E3 activity and sole IBR-RING2 retained the E3 activity (Fig. 4, *light gray circles*), indicating that the second RING finger motif is the catalytic core for the E3 activity of Parkin. Contrary to what was assumed, all disease-relevant mutations other than those in RING2 still possessed E3 activities equivalent to that of the wild-type Parkin (Fig. 4*B*). The same results were observed when UbcH7 or Uev1-Ubc13 was used as E2 (data not shown). In these assays, we used a bacterially expressed recombinant Parkin, and to our knowledge, this is the first direct evidence that E3 activity of the strictly pure Parkin harboring various pathogenic mutations is not compromised.

DISCUSSION

To date, numerous biochemical studies have been performed to understand the E3 activity of Parkin. However, it is difficult to rule out the possible involvement of other E3s (see Introduction). Furthermore, the lack of a good model substrate spurs the difficulty to check the intrinsic E3 activity of Parkin. We thus set up a sensitive E3 assay system using bacterially expressed recombinant Parkin. Our assay system has some advantages; namely, we can obtain a large quantity of MBP-Parkin with higher E3 activity than GST-Parkin (Fig. 1). In addition, this fusion protein was already primed for ubiquitylation even in the absence of model substrate, because fused MBP can work as a good pseudo-substrate (Fig. 2). More importantly, because MBP-Parkin is purified from *E. coli*, it is free from possible contamination of other E3(s). The establishment of this assay allowed us to perform a thorough biochemical characterization of Parkin protein.

Interestingly, sole Parkin catalyzes multiple monoubiquitylation *in vitro* (Fig. 3). Moreover, although Doss-Pepe *et al.* (20) reported that Parkin accelerates polyubiquitin chain formation, the MBP-Parkin in our assay did not stimulate the assembly of polyubiquitin chain (Fig. 1*D*, compare *lanes 4* and *6*, and *10* and *12*, respectively). These results seemingly suggest that the ubiquitylation catalyzed by Parkin functions not for proteasomal degradation but for non-proteasomal-proteolytic function(s), such as transcriptional regulation and/or membrane trafficking *in vivo*. However, it is still premature to make such conclusion. Although we showed that pure Parkin catalyzes multiple monoubiquitylation *in vitro* (Fig. 3), some additional factor(s) like E4 can work together *in vivo*, and this needs to be considered. E4 can extend the ubiquitin chain by recognizing the ubiquitin moiety of a ubiquitylated-protein as a substrate (25). If such an E4-like factor(s) cooperates with Parkin *in vivo*, it is still possible that monoubiquitylation catalyzed by Parkin is used as the scaffold for further polyubiquitylation and finally functions for proteasomal degradation. All things considered, further studies are obviously required; in particular, the authentic substrate and the function of Parkin-catalyzed ubiquitylation need to be addressed.

Another unexpected result was that most of the PD-relevant missense mutations do not abrogate E3 activity of Parkin (Fig. 4). Only missense mutations in the rear RING finger motif abolished the E3 activity, revealing that not the first but the second RING finger motif is the catalytic core of Parkin. Recently, several studies that focused on the pathophysiological mechanisms of Parkin have been published (26–30). Although our results on enzymatic activities of mutant Parkin are not fully consistent with previous reports (see supplemental Table 1), methodological differences in the E3 assay may account for the conflicting observation. For example, in one study immunoprecipitated Parkin was used as the source of E3 *in vitro* (31) and in other studies, E3 activity of Parkin was checked by whether or not coexpression of Parkin in cells enhances the ubiquitylation of the putative substrate (7, 30). Although there is little discrepancy, recent studies and our present work drew the same conclusion that the dysfunction of Parkin is not simply attributable to catalytic impairment of its E3 activity. Indeed, several missense mutations cause Parkin to be sequestered into an aggresome-like structure, and this phenomenon may be involved in disease pathogenesis

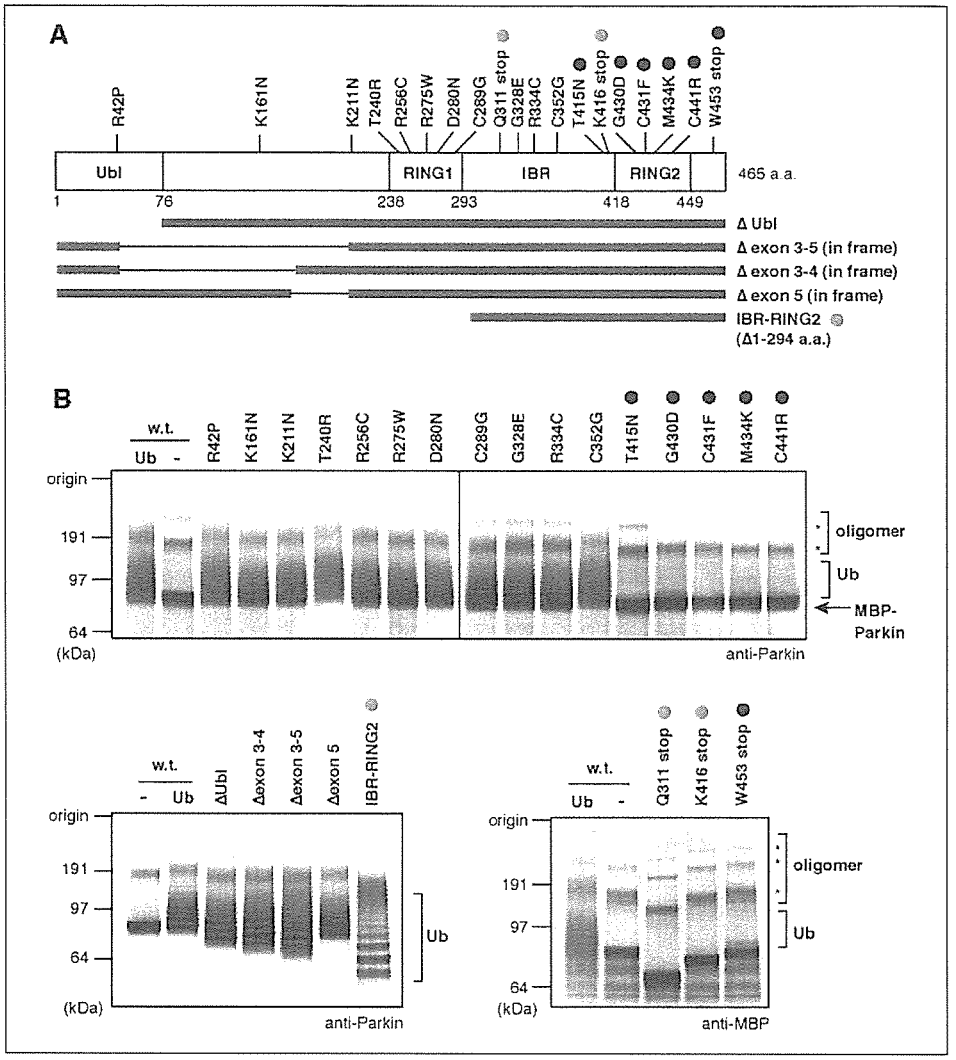

FIGURE 4. *A*, schematic diagram of disease-relevant mutations and exonic deletions of Parkin. *B*, E3 activities of various Parkin proteins bearing PD-linked mutations and deletions. Note that mutations neighboring the second RING finger motif (*solid circles*) abolished E3 activity of Parkin. *Light gray circles* indicate that the RING2 is the catalytic core of Parkin (see text for details). Conversely, pathogenic mutants other than RING2 mutants retain E3 activities equivalent to that of the wild-type (*w.t.*) control. *Ub*, autoubiquitylation; *, oligomerization bands.

(27–30). We think that disease-relevant mutations cause not only attenuation of E3 activity but also a variety of primary defects such as sequestration into aggresome and dissociation from its partner protein, and possibly a complex of such defects may eventually lead to Parkin dysfunction and autosomal recessive juvenile parkinsonism.

PD is the second most prevalent neurodegenerative disorder, and thus, analysis of Parkin is important in terms of public welfare. Indeed, a large number of articles on Parkin have been published; however, because of fierce scientific competition, not all Parkin-related phenomena were critically scrutinized although there remains room for close examination. For example, Pawlyk *et al.* (32) recently inspected the anti-Parkin antibodies and uncovered a high non-specificity of the available Parkin antibodies. This also holds true for the E3 activity of Parkin, because precedent works could not exclude the possible involvement of another E3(s). Herein we investigated thoroughly the enzymatic activity of bacterially expressed recombinant Parkin. Although our work is not conspicuous, we hope that our biochemical characterization using pure Parkin would be a solid cornerstone for further studies, as the preceding works were.

Acknowledgments—We thank Dr. Tsunehiro Mizushima of Nagoya University for providing recombinant Ubc7 protein. We also thank all members of Prof. K. Tanaka laboratory for the helpful discussions.

REFERENCES

1. Moore, D. J., West, A. B., Dawson, V. L., and Dawson, T. M. (2005) *Annu. Rev. Neurosci.* **28,** 57–87
2. Giasson, B. I., and Lee, V. M. (2003) *Cell* **114,** 1–8
3. Ross, C. A., and Pickart, C. M. (2004) *Trends Cell Biol.* **14,** 703–711
4. Tanaka, K., Suzuki, T., Hattori, N., and Mizuno, Y. (2004) *Biochim. Biophys. Acta* **1695,** 235–247
5. Hattori, N., and Mizuno, Y. (2004) *Lancet* **364,** 722–724
6. Lohmann, E., Periquet, M., Bonifati, V., Wood, N. W., De Michele, G., Bonnet, A. M., Fraix, V., Broussolle, E., Horstink, M. W., Vidailhet, M., Verpillat, P., Gasser, T., Nicholl, D., Teive, H., Raskin, S., Rascol, O., Destee, A., Ruberg, M., Gasparini, F., Meco, G., Agid, Y., Durr, A., and Brice, A. (2003) *Ann. Neurol.* **54,** 176–185
7. Ren, Y., Zhao, J., and Feng, J. (2003) *J. Neurosci.* **23,** 3316–3324
8. Corti, O., Hampe, C., Koutnikova, H., Darios, F., Jacquier, S., Prigent, A., Robinson, J. C., Pradier, L., Ruberg, M., Mirande, M., Hirsch, E., Rooney, T., Fournier, A., and Brice, A. (2003) *Hum. Mol. Genet.* **12,** 1427–1437
9. Imai, Y., Soda, M., Hatakeyama, S., Akagi, T., Hashikawa, T., Nakayama, K. I., and Takahashi, R. (2002) *Mol. Cell* **10,** 55–67
10. Zhong, L., Tan, Y., Zhou, A., Yu, Q., and Zhou, J. (2005) *J. Biol. Chem.* **280,** 9425–9430
11. You, J., Cohen, R. E., and Pickart, C. M. (1999) *BioTechniques* **27,** 950–954
12. Matsuda, N., Suzuki, T., Tanaka, K., and Nakano, A. (2001) *J. Cell Sci.* **114,** 1949–1957
13. Imai, N., Matsuda, N., Tanaka, K., Nakano, A., Matsumoto, S., and Kang, W. (2003) *J. Virol.* **77,** 923–930
14. Matsuda, N., Azuma, K., Saijo, M., Iemura, S., Hioki, Y., Natsume, T., Chiba, T., Tanaka, K., and Tanaka, K. (2005) *DNA Repair (Amst.)* **4,** 537–545
15. Shimura, H., Hattori, N., Kubo, S., Yoshikawa, M., Kitada, T., Matsumine, H., Asakawa, S., Minoshima, S., Yamamura, Y., Shimizu, N., and Mizuno, Y. (1999) *Ann.*

Neurol. **45,** 668–672
16. Rankin, C. A., Joazeiro, C. A., Floor, E., and Hunter, T. (2001) *J. Biomed. Sci.* **8,** 421–429
17. Araki, K., Kawamura, M., Suzuki, T., Matsuda, N., Kanbe, D., Ishii, K., Ichikawa, T., Kumanishi, T., Chiba, T., Tanaka, K., and Nawa, H. (2003) *J. Neurochem.* **86,** 749–762
18. Takai, R., Matsuda, N., Nakano, A., Hasegawa, K., Akimoto, C., Shibuya, N., and Minami, E. (2002) *Plant J.* **30,** 447–455
19. Hofmann, R. M., and Pickart, C. M. (1999) *Cell* **96,** 645–653
20. Doss-Pepe, E. W., Chen, L., and Madura, K. (2005) *J. Biol. Chem.* **280,** 16619–16624
21. Lim, K. L., Chew, K. C., Tan, J. M., Wang, C., Chung, K. K., Zhang, Y., Tanaka, Y., Smith, W., Engelender, S., Ross, C. A., Dawson, V. L., and Dawson, T. M. (2005) *J. Neurosci.* **25,** 2002–2009
22. Chen, Z. J. (2005) *Nat. Cell Biol.* **7,** 758–765
23. Hicke, L. (2001) *Nat. Rev. Mol. Cell Biol.* **2,** 195–201
24. Pickart, C. M. (2000) *Trends Biochem. Sci.* **25,** 544–548
25. Richly, H., Rape, M., Braun, S., Rumpf, S., Hoege, C., and Jentsch, S. (2005) *Cell* **120,** 73–84
26. Cookson, M. R., Lockhart, P. J., McLendon, C., O'Farrell, C., Schlossmacher, M., and Farrer, M. J. (2003) *Hum. Mol. Genet.* **12,** 2957–2965
27. Gu, W. J., Corti, O., Araujo, F., Hampe, C., Jacquier, S., Lucking, C. B., Abbas, N., Duyckaerts, C., Rooney, T., Pradier, L., Ruberg, M., and Brice, A. (2003) *Neurobiol. Dis.* **14,** 357–364
28. Henn, I. H., Gostner, J. M., Lackner, P., Tatzelt, J., and Winklhofer, K. F. (2005) *J. Neurochem.* **92,** 114–122
29. Wang, C., Tan, J. M., Ho, M. W., Zaiden, N., Wong, S. H., Chew, C. L., Eng, P. W., Lim, T. M., Dawson, T. M., and Lim, K. L. (2005) *J. Neurochem.* **93,** 422–431
30. Sriram, S. R., Li, X., Ko, H. S., Chung, K. K., Wong, E., Lim, K. L., Dawson, V. L., and Dawson, T. M. (2005) *Hum. Mol. Genet.* **14,** 2571–2586
31. Staropoli, J. F., McDermott, C., Martinat, C., Schulman, B., Demireva, E., and Abeliovich, A. (2003) *Neuron* **37,** 735–749
32. Pawlyk, A. C., Giasson, B. I., Sampathu, D. M., Perez, F. A., Lim, K. L., Dawson, V. L., Dawson, T. M., Palmiter, R. D., Trojanowski, J. Q., and Lee, V. M. (2003) *J. Biol. Chem.* **278,** 48120–48128

doi:10.1016/j.jmb.2005.11.018 J. Mol. Biol. (2006) 355, 612–618

JMB

Available online at www.sciencedirect.com

SCIENCE DIRECT®

ELSEVIER

COMMUNICATION

The Crystal Structure of Human Atg4b, a Processing and De-conjugating Enzyme for Autophagosome-forming Modifiers

Taichi Kumanomidou[1], Tsunehiro Mizushima[1,2], Masaaki Komatsu[3,4] Atsuo Suzuki[1], Isei Tanida[4], Yu-shin Sou[4], Takashi Ueno[4] Eiki Kominami[4], Keiji Tanaka[3]* and Takashi Yamane[1]*

[1]*Department of Biotechnology Graduate School of Engineering Nagoya University, Chikusa-ku Nagoya 464-8603, Japan*

[2]*PRESTO, Japan Science and Technology Agency, Kawaguchi Saitama 332-0012, Japan*

[3]*Laboratory of Frontier Science Tokyo Metropolitan Institute of Medical Science, Bunkyo-ku Tokyo 113-8613, Japan*

[4]*Department of Biochemistry Juntendo University School of Medicine, Bunkyo-ku, Tokyo 113-8421, Japan*

**Corresponding authors*

Autophagy is an evolutionarily conserved pathway in which the cytoplasm and organelles are engulfed within double-membrane vesicles, termed autophagosomes, for the turnover and recycling of these cellular constituents. The yeast Atg8 and its human orthologs, such as LC3 and GABARAP, have a unique feature as they conjugate covalently to phospholipids, differing from ubiquitin and other ubiquitin-like modifiers that attach only to protein substrates. The lipidated Atg8 and LC3 localize to autophagosomal membranes and play indispensable roles for maturation of autophagosomes. Upon completion of autophagosome formation, some populations of lipidated Atg8 and LC3 are delipidated for recycling. Atg4b, a specific protease for LC3 and GABARAP, catalyzes the processing reaction of LC3 and GABARAP precursors to mature forms and de-conjugating reaction of the modifiers from phospholipids. Atg4b is a unique enzyme whose primary structure differs from that of any other proteases that function as processing and/or de-conjugating enzymes of ubiquitin and ubiquitin-like modifiers. However, the tertiary structures of the substrates considerably resemble that of ubiquitin except for the N-terminal additional domain. Here we determined the crystal structure of human Atg4b by X-ray crystallography at 2.0 Å resolution, and show that Atg4b is a cysteine protease whose active catalytic triad site consists of Cys74, His280 and Asp278. The structure is comprised of a left lobe and a small right lobe, designated the "protease domain" and the "auxiliary domain", respectively. Whereas the protease domain structure of Atg4b matches that of papain superfamily cysteine proteinases, the auxiliary domain contains a unique structure with yet-unknown function. We propose that the R229 and W142 residues in Atg4b are specifically essential for recognition of substrates and catalysis of both precursor processing and de-conjugation of phospholipids.

Keywords: Atg4b; autophagy; ubiquitin-like modifier; cysteine protease; tertiary structure

There is growing evidence regarding the importance of ubiquitin (Ub) and ubiquitin-like proteins (Ubls) as landmark molecules of new type post-translational protein-modifying systems responsible for diverse cellular activities, such as intracellular protein proteolysis and other non-proteolytic roles in eukaryotic cells.[1–3] Ub and Ubls are covalently attached to client molecules by an elaborate cascade system consisting of activating (E1), conjugating (E2), and/or ligating (E3) enzymes. Intriguingly, Ub is encoded by two types

Abbreviations used: Ub, ubiquitin; Ubl, ubiquitin-like protein; GABARAP, gamma-aminobutyric-acid type-A receptor-associated protein; PE, phosphatidylethanolamine.

E-mail addresses of the corresponding authors: tanakak@rinshoken.or.jp; yamane@nubio.nagoya-u.ac.jp

of unique genes; a poly(Ub) gene, which encodes a tandemly repeated Ub (so-called "heat-shock gene"), and an Ub-fused gene with certain ribosomal proteins of unknown biological significance.[4,5] In addition, some Ubl modifiers (if not all) are also synthesized in precursor forms with extension adducts (consisting of several amino acid residues) in the COOH-termini. The Ub-fused proteins and the extra adducts of Ubls must be cleaved prior to their conjugation to target molecules. It is noteworthy that most of these Ub and Ubl-modifying reactions are reversible; i.e. Ub/Ubl-conjugates are de-conjugated from the substrates to abolish the effects of modifications, and then the Ub/Ubl modifiers are re-utilized for other cycles of respective modifications.[6] For these events, various enzymes catalyze the maturation of precursor modifiers (i.e. reactions that produce functional Ub or Ubl moieties from their precursor forms) and de-conjugation of Ub or Ubl-ligated molecules in eukaryotic cells. These enzymes belong to a large protein family of cysteine proteases, with the exception of certain de-ubiquitinating enzymes that are metalloproteases.[7]

Human Atg4b, the yeast Atg4 homologue essential for autophagy, cleaves the COOH-terminal adducts of microtubule-associated protein 1 light chain 3 (LC3) and gamma-aminobutyric-acid type-A receptor-associated protein (GABARAP), a human Atg8 ortholog.[8,9] Among the Ubl modifiers, the yeast Atg8 and its human orthologs have a unique feature in that they conjugate covalently to phospholipids such as phosphatidylethanolamine (PE), thus differing from any other ubiquitin-like modifiers that conjugate only to protein substrates.[8–10]In this regard, the Atg8/LC3 conjugation system to phospholipids is essential for autophagy, a membrane trafficking mechanism that delivers cytoplasmic constituents into the lysosome/vacuole for bulk protein degradation.[11,12] The initial step of autophagy is elongation of the isolation membrane. The isolation membrane enwraps cytoplasmic components including organelles, and then its edges fuse with each other forming a double membrane structure called autophagosome. Finally, the outer membrane of the autophagosome fuses to the lysosome/vacuole and the sequestered cytoplasmic constituents are degraded by the lysosomal/vacuolar hydrolases, together with the inner membrane of the autophagosomes.[13] In this process, the processing of LC3 by Atg4b is essential for LC3-lipidation during autophagosome formation. Lipidated LC3 localizes to autophagosomes and some populations are delipidated by Atg4b after autophagosome maturation for recycling.[9,14] Considering the specific function of Atg8/LC3 family proteins, it is necessary to determine the structure of this processing/de-conjugating enzyme, Atg4b. Here we report for the first time the tertiary structure and the substrate recognition mechanism of Atg4b and compare these properties to those of other de-ubiquitylating enzymes and structurally similar proteases.

Overall structure of Atg4b

The structure determination process is summarized in Table 1. Atg4b adapts an α/β structure with overall dimensions of 60 Å × 55 Å × 50 Å consisting of 13 β-strands designated β1–β13, eight α-helices (α1–α8) and three 3_{10} helices. The 3_{10}–1 helix is located at the N-terminal region, 3_{10}–2 is in the loop between β10 and β11, and 3_{10}–3 is in between β11 and β12. Atg4b is composed of a left lobe and a small right lobe, designated the "protease domain" and the "auxiliary domain", respectively (Figure 1(a)). The structure from residues 191 to 215, which links the auxiliary domain and protease domain, could not be constructed because of the weak electron density. Despite the lack of obvious sequence homology to papain, the protease domain of Atg4b matches that of papain superfamily cysteine proteases. Superposition of Atg4b with papain on the 119 C^{α} atoms of the optimal Atg4b–papain overlap resulted in a root-mean-square deviation (r.m.s.d.) of 2.1 Å (Figure 1(b)). The secondary structure elements of the central antiparallel β-sheet (β11, β9, β8, β7, β12 and β6) and helix α2 are structurally equivalent to those of papain-like proteases (Figure 1(c)). The protease domain of Atg4b is divided into two distinct subdomains and the active site of Atg4b is located between the two sub-domains (Figure 1(a) and (c)). On the other hand, the auxiliary domain contains two β-strands and two α-helices, in which the papain superfamily does not hold (Figure 1(b)). The auxiliary domain may provide additional functions, such as substrate recognition.

The structure of Atg4b was compared with those of other proteins in the PDB database using the DALI server.[15] Atg4b is structurally similar to a cysteine protease, IdeS (PDB ID code 1y08),[16] with a r.m.s.d. value of 3.8 Å. IdeS is also an endopeptidase with uniquely high specificity. This protease recognizes the L-L-G-G motif in IgG. Comparison of the primary structures of Atg4b and IdeS showed an homology of approximately 20%.

Mechanism of catalysis

A decrease in enzymatic activity after mutation of residues H280 and D278 indicates that these amino acid residues form a catalytic triad (data not shown). The active site cysteine, C74, histidine and aspartate residues are well conserved in all known Atg4 sequences.[17] The active site of Atg4b is located at the N-terminal region of helix α2 and the loop connecting strands β9 and β10. The active site of Atg4b fits the corresponding residues in UCH-L3,[18] papain,[19] cathepsin B,[20] and HAUSP[21] (Figure 2(a)). The hydrogen bond network between Atg4b and others is essentially the same. However, the orientation of the imidazole ring of H280 of Atg4b is clearly different from those of other cysteine proteases. The C^{α} position of H280 in Atg4b is located on the opposite side of the active site H159 in papain.[19] The structural similarity at

Table 1. Data collection, phasing and refinement statistics

	Native 1	Native 2	Thimerosal	Hg $(CH_3COO)_2$	Pb $(CH_3COO)_2$	$IrCl_3$	K_2PtCl_6
A. *Data collection*							
Space group	$P2_1$	$P2_1$	–	–	–	–	–
Resolution (Å)	2.0	2.0	2.4	3.3	2.4	2.6	2.8
Observations	180,458	114,063	122,583	40,417	86,164	76,675	40,579
Unique reflections	48,166	39,483	27,747	10,816	24,628	20,857	16,168
Completeness (%) (last shell)	98.7 (99.1)	81.5 (73.2)	98.5 (98.6)	99.8 (100.0)	88.6 (81.6)	95.0 (100.0)	92.4 (96.1)
Redundancy	3.7 (3.3)	2.9 (2.4)	4.4 (4.1)	3.7 (3.8)	3.6 (3.3)	3.7 (3.8)	2.5 (2.5)
R_{sym} (%) (last shell)	3.0 (16.3)	3.7 (30.7)	5.6 (19.3)	7.0 (27.6)	3.9 (28.6)	3.9 (19.9)	5.8 (28.0)
I/σ	23.8	19.5	16.6	12.2	17.8	18.2	12.6
B. *MIRAS phasing*							
Resolution (Å)	–	–	2.4	3.3	2.4	2.6	2.8
R_{iso} *versus* Native 2	–	–	0.199	0.195	0.155	0.106	0.108
Heavy atom sites	–	–	9	3	4	4	3
Phasing power (anomalous)	–	–	1.486 (1.055)	0.016 (0.008)	0.062 (0.032)	0.079 (0.035)	0.022 (0.009)
R_{cullis} (anomalous)	–	–	0.608 (0.803)	0.835 (0.912)	0.699 (0.959)	0.603 (0.945)	0.867 (1.000)
C. *Refinement statistics*							
Resolution range (Å)	45.0–2.00	–	–	–	–	–	–
Reflections	45,690	–	–	–	–	–	–
Protein atoms	5386	–	–	–	–	–	–
Solvent	337	–	–	–	–	–	–
R_{cryst}/R_{free} (%)	22.0/28.3	–	–	–	–	–	–
D. *r.m.s.d. from ideal values*							
Bond length (Å)	0.011	–	–	–	–	–	–
Bond angle (deg.)	1.42	–	–	–	–	–	–
Ramachandran plot							
Most favored (%)	87.6	–	–	–	–	–	–
Additionally allowed (%)	10.3	–	–	–	–	–	–
Generously allowed (%)	2.1	–	–	–	–	–	–

The full-length human Atg4b was cloned into pGEX-6P (Amersham Biosciences). For overexpression in *E. coli*, the recombinant plasmid was transformed into BL21 (RIL) (Novagen). Protein expression was induced at 35.5 °C with 0.1 mM isopropyl-β-D-thiogalactoside. After further growth for 4 h, the bacteria were pelleted, resuspended in 20 mM Tris–HCl (pH 7.4) and 150 mM NaCl, and lysed by sonication. The resulting soluble fraction was purified using glutathione Sepharose 4B and anion exchange chromatography. The GST moiety was proteolytically removed by PreScission protease. Crystals of Atg4b were obtained at 15°C by the hanging-drop vapor-diffusion method, with a mixture of 2.0 μl of protein (6.8 mg/ml) in buffer containing 25 mM Tris–HCl (pH 7.5), 1 mM dithiothreitol (DTT), and the same volume of reservoir solution (0.65–0.70 M sodium citrate (pH 6.5)). The crystals belong to the space group $P2_1$, with $a=51.28$ Å, $b=161.32$ Å, $c=51.27$ Å, and $\beta=119.6°$. There are two molecules per asymmetric unit. The crystals were equilibrated in a cryo-protectant buffer containing reservoir buffer plus 10%(v/v) glycerol and then frozen in a cold nitrogen stream at 100 K. Heavy-atom soaks were performed in crystallization buffer with 0.01 mM thimerosal (22 h), 0.01 mM $Hg(CH_3COO)_2$ (7 min), $Pb(CH_3COO)_2$ (22 h), $IrCl_2$ (18 h) and K_2PtCl_6 (22 h). All data sets were collected on beamline BL44XU at Spring-8, and processed using the software Denzo and Scalepack and programs from CCP4 package. The structure of Atg4b was determined using Native 2 dataset by the multiple isomorphous replacement anomalous scattering (MIRAS) method. Atomic positions for heavy-atoms in the asymmetric unit were determined by using SHELXD[26] and refined by using SHARP. Initial MIRAS phases were extended to 2.0 Å and improved with solvent flattening and histogram matching using DM. The initial model was constructed with the program ARP/wARP.[27] Atg4b crystals showed low isomorphism between different native crystals. The final Atg4b structure was determined using Native 2 dataset with high completeness by the molecular replacement technique. As the search model, the initial model was applied. The warpNtrace mode of ARP/wARP then built a model automatically, which had 570 of the 786 amino acid residues of Atg4b in the native electron density at a resolution of 2.0 Å. The remaining parts of the structure were built manually using the program XtalVIew.[28] The model was refined at 2.0 Å resolution using the program REFMAC5.[29] The final refined model contained two molecules. Both models contained residues 10–190 and 216–373. The Table lists the methods used for data collection and phasing and refinement statistics. Data for the outer shell are in parentheses.

the active sites suggests that the catalytic mechanism of Atg4b is similar to that of papain. In Atg4b, C74 and H280 form a thiolate imidazolium ion pair, and D278 functions to orient the active site residues correctly and stabilizes the protonated form of H280, while Y54 plays a role in the oxyanion hole. Comparison of the surface representations of both enzymes revealed that both active site clefts are formed between two distinct sub-domains (Figure 2(b)). While the active site cleft of papain is open and allows accessing the substrate, the corresponding active site cleft of Atg4b is closed by lid loop of the enzyme. The lid loop (residues 258–263, especially N261) connecting β7 and β8 covers the active site C74 though it is flexible because of the residues' high temperature factors (Figure 3(a) and (b)). Indeed, the hydrogen bond network between N261 and the active site residue is observed *via* a water molecule (Figure 3(b)). The scheme of the hydrogen bonds is N261···Wat49, Wat49···C74 and Wat49···Y54. Notably, the space for substrate binding is very small in the active site, suggesting a closed structure, corresponding to a self-inhibited state. This conformation is not likely to be

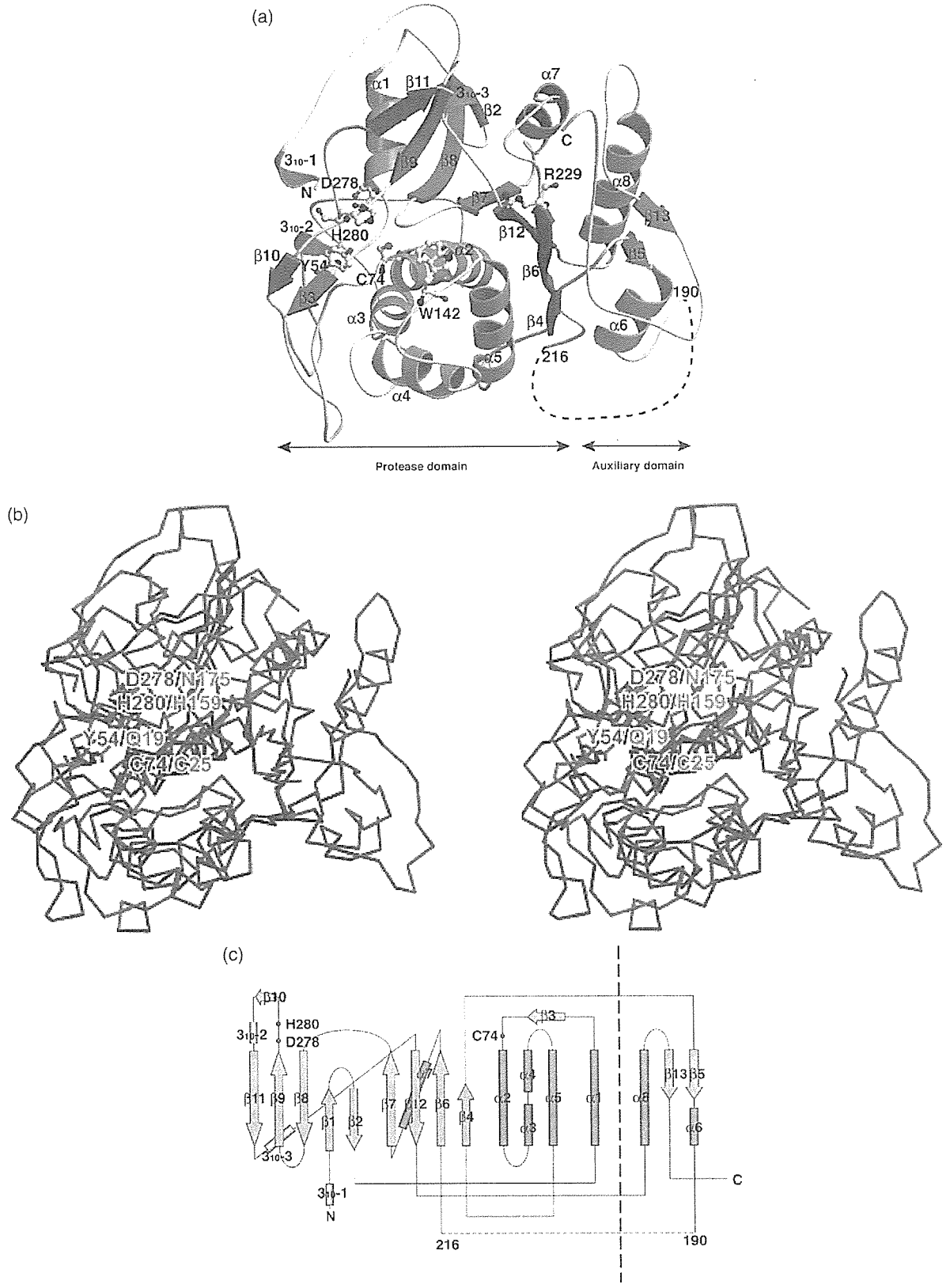

Figure 1. (a) Schematic drawing of Atg4b. The color codes for the secondary structure elements are: α-helix, cyan; β-strands, magenta; loops, salmon. The active site residues Y54, C74, W142, R229, D278 and H280 are shown in ball-and-stick representation. (b) Stereo diagram showing the superposition of C^{α} of Atg4b (blue) and papain (red). (For 119 aligned C^{α} atoms, r.m.s.d. = 2.1 Å.) (c) A topology diagram of Atg4b. The α-helices appear as cyan-colored cylinders and are labeled α1–α8. The β-strands appear as magenta-colored arrows and are labeled β1–β13. The 3_{10} helices appear as gray-colored cylinders and are labeled 3_{10}–1–3_{10}–3. Red circles indicate the positions of the active site residues.